Available online at www.sciencedirect.com

SciVerse ScienceDirect

Geochimica et Cosmochimica Acta 115 (2013) 217–240

Geochimica et Cosmochimica Acta

www.elsevier.com/locate/gca

A geochemical model of non-ideal solutions in the methane–ethane–propane–nitrogen–acetylene system on Titan

Christopher R. Glein [a,*], Everett L. Shock [a,b]

[a] School of Earth and Space Exploration, Arizona State University, Tempe, AZ 85287-1404, United States
[b] Department of Chemistry and Biochemistry, Arizona State University, Tempe, AZ 85287-1604, United States

Received 19 November 2012; accepted in revised form 23 March 2013; available online 8 April 2013

Abstract

Saturn's largest moon, Titan, has an atmosphere and surface that are rich in organic compounds. Liquid hydrocarbons exist on the surface, most famously as lakes. Photochemical reactions produce solid organics in Titan's atmosphere, and these materials settle or snow onto the surface. At the surface, liquids can interact with solids, and geochemical processes can occur. The consequences of these processes can be explored using a thermodynamic model to calculate the solubilities of gases and solids in liquid hydrocarbons at cryogenic temperatures. The van Laar model developed in this study was parameterized using experimental phase equilibrium data, and accurately represents the data for the CH_4–C_2H_6–C_3H_8–N_2–C_2H_2 chemical system from 90 to 110 K. The model generally gives more accurate results than existing models. The model also features a suitable balance between accuracy and simplicity, and can serve as a foundation for studies of fluvial geochemistry on Titan because it can be extended to any number of components while maintaining thermodynamic consistency. Application of the model to Titan reveals that the equilibrium composition of surface liquids depends on the abundance of methane gas in the local atmosphere, consistent with prior studies. The concentration of molecular nitrogen in Titan's lakes varies inversely with the ethane content of the lakes. The model indicates that solid acetylene should be quite soluble in surface liquids, which implies that acetylene-rich sedimentary rocks would be susceptible to chemical erosion, and acetylene evaporites may form on Titan. The geochemical character of acetylene in liquid hydrocarbons on Titan appears to be intermediate to those of calcite and gypsum in surface waters on Earth. Specific recommendations are given of observational, experimental, and theoretical work that will lead to significant advancements in our knowledge of geochemical processes on Titan. This paper represents the beginning of a new kind of geochemistry, called cryogenic fluvial geochemistry, with Titan starring as the first example.

1. INTRODUCTION

Saturn's giant satellite, Titan, is a frigid but not entirely frozen world as there is extensive evidence for the presence of surface liquids that erode the land (see reviews by Jaumann et al., 2009; Lunine & Lorenz, 2009). Global observations by the Titan Radar Mapper instrument onboard the Cassini spacecraft have revealed ubiquitous channels with diverse morphologies (e.g., branching, meandering, braiding) that are indicative of fluvial transport and erosion (Elachi et al., 2006; Lorenz et al., 2008a; Langhans et al., 2012). The longest channels have lengths of several hundred kilometers. By analogy with Earth, the presence of dendritic networks of valleys implies that rivers are supplied by a distributed source of rainfall, presumably with a methane-rich composition (Lorenz et al., 2008a) based on the facts that methane (CH_4) is the second most abundant constituent of Titan's atmosphere (Niemann et al., 2010), and liquid

* Corresponding author. Present address: Geophysical Laboratory, Carnegie Institution of Washington, 5251 Broad Branch Road NW, Washington, DC 20015-1305, United States. Tel.: +1 480 620 6465; fax: +1 202 478 8901.
E-mail address: cglein@ciw.edu (C.R. Glein).

0016-7037/$ - see front matter © 2013 Elsevier Ltd. All rights reserved.
http://dx.doi.org/10.1016/j.gca.2013.03.030

CH_4 is volatile enough to participate in a cycle that is analogous to the hydrologic cycle on Earth (in contrast to liquid ethane). Changes in surface brightness after a cloud outburst also provide indirect evidence for recent rainfall near Titan's equator (Turtle et al., 2011a).

The Titan Radar Mapper has also revealed surface features that are regarded as lakes or seas of liquid hydrocarbons (Stofan et al., 2007; Hayes et al., 2008; Turtle et al., 2009; Stephan et al., 2010). These features are radar-dark, which implies that they have smooth surfaces; they have shapes that resemble various types of lakes on Earth; and some of the features are associated with sinuous channels (presumably rivers feeding the lakes). Observed lakes and seas are generally restricted to Titan's polar regions, and they are more abundant in the north polar region than in the south (Aharonson et al., 2009). The largest seas have surface areas of several hundred square kilometers. Infrared spectroscopic data obtained by the Visual and Infrared Mapping Spectrometer (VIMS) on Cassini strongly suggest the presence of liquid ethane (C_2H_6) in the south polar lake Ontario Lacus (Brown et al., 2008).

In addition, data from the Huygens probe provide localized evidence of fluvial processes on Titan. Dendritic valley networks draining from highlands to lowlands were observed during the descent of the probe (Soderblom et al., 2007), and the Huygens landing site was peppered with rounded stones, which may have been abraded during earlier fluvial transport (Tomasko et al., 2005). Some liquid CH_4 and C_2H_6 appeared to be present at the landing site, because the abundances of gaseous CH_4 and C_2H_6 increased when surface material was heated, presumably as a result of evaporation (Niemann et al., 2010).

These discoveries incite many questions pertaining to geochemistry. What are the chemical compositions of surface liquids on Titan? How chemically complex and diverse are the molecules dissolved in such liquids? What physical and chemical processes control liquid composition, and how do they operate over space and time? How soluble are atmospheric gases and surface solids in liquids on Titan? Does chemical weathering occur? Are there geological features that are produced by processes involving the dissolution or precipitation of solids? How does fluvial geochemistry on Titan compare to that on Earth (and Mars)? While definitive answers to these questions must await future spacecraft exploration (e.g., Coustenis et al., 2009; TSSM Final Report, 2009; Stofan et al., 2010), preparations for future missions will be enhanced by formulating hypotheses that can be tested experimentally and theoretically. A group at the Jet Propulsion Laboratory is measuring the solubilities of organic solids and noble gases in liquid hydrocarbons at cryogenic conditions (Hodyss et al., 2010, 2012; see also Diez y Riega, 2010). The time seems ripe to initiate a complementary program of theoretical research on equilibrium geochemistry. Thus, the primary goal of the present study is to develop a model that can be used to describe quantitatively thermodynamic equilibria among gas, liquid, and solid phases on Titan. Knowledge of chemical equilibrium is powerful, as experience demonstrates that many geochemical phenomena on Earth can be understood in terms of equilibrium concepts (e.g., Garrels and Christ, 1965; Drever, 1997). Characterization of equilibrium is also the first step toward identifying departures from equilibrium and processes that create disequilibria.

Several equilibrium composition models have been developed for applications to Titan (Lunine et al., 1983; Lunine, 1985; Thompson, 1985; Raulin, 1987; Dubouloz et al., 1989; Thompson et al., 1990, 1992; Gabis, 1991; Kouvaris and Flasar, 1991; Cordier et al., 2009, 2010, 2012; Heintz and Bich, 2009; Tan et al., 2013). While these studies were trailblazing in drawing attention to aspects of Titan's geochemistry, a new, geochemically oriented model is needed because existing models are too highly parameterized to specific chemical systems, too complex for routine geochemical calculations, or insufficiently accurate relative to the quality of data now available from Titan. In many cases, earlier models were not tested by explicit comparison with experimental data, which leads to questions about how well the models perform. In some cases, model parameters or other input data are not provided. At present, significant uncertainties are encountered when existing models are used to study fluvial geochemistry on Titan. Accordingly, an objective of the study presented here was to develop a generalized thermodynamic framework that is both accurate and easy-to-use. Our geochemical model is built from internally consistent thermodynamic data, and is tested by explicit comparison with experimental data. Another goal of the present study was to identify similarities and differences between aqueous geochemistry on Earth and hydrocarbon geochemistry on Titan. The terrestrial context helps in relating output from thermodynamic modeling to the occurrences and behaviors of materials, and associated geological processes on Titan.

The purpose of this communication is to present an empirical model that represents, as accurately as possible, solid–liquid–vapor phase equilibrium between CH_4, C_2H_6, C_3H_8 (propane), N_2 (molecular nitrogen), and C_2H_2 (acetylene) at Titan surface conditions. N_2 and CH_4 are the major constituents of Titan's atmosphere (Niemann et al., 2010), and C_2H_6, C_2H_2, and C_3H_8 are the three most abundant products of CH_4 photochemistry in the atmosphere (Magee et al., 2009; Coustenis et al., 2010; Vinatier et al., 2010). Transport (e.g., diffusion, turbulent mixing) and condensation processes in Titan's atmosphere deliver these compounds and others to the surface (Strobel et al., 2009), where they can participate in geochemical processes (Lorenz and Lunine, 1996). Photochemical models (e.g., Yung et al., 1984; Lavvas et al., 2008a,b) predict that large quantities of liquid C_2H_6 and solid C_2H_2 (along with smaller amounts of liquid C_3H_8) would have accumulated on Titan's surface if present-day photochemical production rates are applicable to Titan's past (Lunine et al., 1983). However, a preliminary survey of Titan's lakes suggested that there may be less C_2H_6 than originally thought (Lorenz et al., 2008b). Similarly, C_2H_2 may not be as ubiquitous as once believed, as VIMS has not detected it thus far (Clark et al., 2010). On the other hand, C_2H_2 was detected *in situ* by the Huygens Gas Chromatograph–Mass Spectrometer (GC–MS; Niemann et al., 2010). The CH_4–C_2H_6–C_3H_8–N_2–C_2H_2 system is a relevant and manageable

foundation for a model of fluvial geochemistry on Titan, given that this system features the most important liquid hydrocarbons, arguably the most abundant organic solid, and the dominant atmospheric species on Titan.

In the following sections, we present the thermodynamics of our geochemical model (Section 2), derive model parameters by regression and correlation analyses (Section 3), test the model and alternative models by comparing model predictions to independent experimental data (Section 4), and illustrate how our model can be used to obtain fundamental information about cryogenic hydrocarbon geochemistry on Titan (Section 5). We conclude this paper by making several suggestions for future studies in Section 6.

2. THERMODYNAMIC RELATIONS

Phase equilibrium occurs when the temperature, pressure, and chemical potentials of system components are the same in equilibrating phases. Fugacities (f) are more convenient variables than chemical potentials in thermodynamic modeling, as fugacities are proportional to partial pressures. In terms of fugacities, the phase equilibrium requirement is that the fugacities of system components be equal in equilibrating phases

$$f_k^{\alpha} = f_k^{\beta}, \tag{1}$$

where k designates component k, and α and β stand for separate phases. Standard states (denoted by the $^\circ$ symbol) of temperature, pressure, and composition provide initial conditions for integrating thermodynamic functions to the desired state of the system. Here, we adopt the conventional standard states of pure liquids and solids at the temperature and pressure of interest, and ideal gases at the temperature of interest and a pressure of 1 bar. The standard state for a liquid will be hypothetical if the temperature is below the triple-point temperature, but this is acceptable provided that the fugacity of the hypothetical liquid can be calculated.

Fugacities can be expressed as the product of the standard state fugacity (f°) and the activity (a). For liquids and solids, activity is defined as $a = \gamma x$, where γ signifies the rational activity coefficient, and x represents the mole fraction of the component of interest; for gases, activity is defined as $a = \phi p$, where ϕ refers to the fugacity coefficient, and p corresponds to the partial pressure of the component of interest.

2.1. Vapor–liquid equilibrium

Eq. (1) can be transformed into a form that is useful for modeling vapor–liquid equilibria (Prausnitz et al., 1999), that is

$$(\phi_k p_k f_k^{\circ})^{\mathrm{gas}} = (\gamma_k x_k f_k^{\circ})^{\mathrm{liq}}. \tag{2}$$

Raoult's law can be derived from Eq. (2) by assuming that $\phi_k = \gamma_k = 1$ (i.e., ideal behavior). Real solutions may approximate ideal behavior if the pressure is low, and liquid-phase molecules are similar in size, shape, and chemical nature.

A major goal here is to calculate the solubility of atmospheric gases, such as N_2, in liquids on Titan, which means that x_k must be obtained from Eq. (2). The other five quantities in Eq. (2) are specified using the following strategy. First, $f_k^{\circ,\mathrm{gas}}$ is set to 1 bar, following standard state conventions. Standard state fugacities of liquids ($f_k^{\circ,\mathrm{liq}}$) are computed using the National Institute of Standards and Technology (NIST) REFPROP program (Lemmon et al., 2010), which computes thermodynamic properties using equations of state for the Helmholtz energy (CH_4: Setzmann and Wagner, 1991; C_2H_6: Bucker and Wagner, 2006; C_3H_8: Lemmon et al., 2009; N_2: Span et al., 2000). The equations in REFPROP were optimized to fit a large amount of thermal and volumetric data, and they are accurate but complex. Fugacity coefficients (ϕ_k) are also obtained from REFPROP. Partial pressures of gases (p_k) are treated as free parameters to be compared with analytical data. This leaves the activity coefficients (γ_k).

Typically, rational activity coefficients are obtained from a model that has been shown to be consistent with experimental data. The general procedure is to adopt an activity coefficient model that contains empirical parameters, and then determine best-fit values of the parameters by regressing experimental data. A desirable model would have the following features: (1) a theoretical underpinning; (2) the ability to reproduce experimental data closely; (3) a minimal number of adjustable parameters; (4) options to extend the model to multicomponent systems using binary parameters only; and (5) mathematical simplicity. After considering several options, we concluded that a modified van Laar (MVL) model (van Laar, 1906) satisfies these criteria best. Activity coefficients from this model can be written as (see Appendxi A)

$$RT \times \ln(\gamma_k^{\mathrm{liq}}) = -\sum_{i=1}^{n-1}\sum_{j>i}^{n} \frac{\omega_{ij}\lambda_i\lambda_j q_k}{q_i + q_j}, \tag{3}$$

where R corresponds to the molar gas constant (8.314462 J mol^{-1} K^{-1}; CODATA, 2010), T represents absolute temperature, ω_{ij} denotes the interaction energy for binary system i–j, and q stands for the effective volume of the component of interest in the liquid mixture (note that ratios of q's rather than individual values are important in Eq. (3); see below). Auxiliary function λ depends on the effective volume fraction (z) as $\lambda_i = 1 - z_i$ when $i = k$, or $\lambda_i = -z_i$ when $i \neq k$. Effective volume fractions can be evaluated from

$$z_k = \frac{x_k q_k}{q_{\mathrm{mix}}}, \tag{4}$$

where

$$q_{\mathrm{mix}} = \sum_{i=1}^{n} x_i q_i. \tag{5}$$

The present MVL model was derived (see Appendxi A) from the regular solution theory of Hildebrand (1927) and Scatchard (1931), which is a generalization of van Laar's original theory (see Prausnitz et al., 1999). The difference between our MVL model and Scatchard–Hildebrand theory is that the energy and volume terms in the

regular-solution equations are replaced by empirical parameters. This leads to better agreement with experimental data. Other researchers have also modified van Laar's theory by introducing empirical parameters, including Wohl (1946), Black (1958), Chien and Null (1972), Focke (2001), Holland and Powell (2003), and Peng (2010). In general, the various van Laar-type models are functionally equivalent, and they differ by how energy and volume parameters are defined. For example, the present model is nearly identical to that of Holland and Powell (2003), as Eq. (3) differs from its counterpart in Holland and Powell (2003) by a factor of two.

For future reference, the MVL model gives the following expressions for the activity coefficients in a binary mixture of components 1 and 2

$$RT \times \ln(\gamma_1) = \left(\frac{\omega_{12}}{1+\frac{q_2}{q_1}}\right)\left(1+\frac{q_1 x_1}{q_2 x_2}\right)^{-2}, \quad (6)$$

and

$$RT \times \ln(\gamma_2) = \left(\frac{\omega_{12}}{1+\frac{q_1}{q_2}}\right)\left(1+\frac{q_2 x_2}{q_1 x_1}\right)^{-2}. \quad (7)$$

There are two obstacles to using the above equations. First, the model requires two empirical parameters for each binary system (q_1/q_2 and ω_{12}). This makes it difficult to regress experimental solid–liquid equilibrium data, which generally consist of a single point (i.e., solubility) at a given temperature. Second, the model implicitly relies upon a restrictive relationship between the ratios of q's in multicomponent systems. As an example, ternaries must obey the relationship $(q_3/q_2) = (q_3/q_1) \times (q_1/q_2)$ for the model to maintain mathematical consistency (Wohl, 1946). This limitation is undesirable because some systems may not satisfy the relationship. A way forward is to replace q ratios with ratios of actual volumes. Two candidates are liquid volume ratios (Hildebrand and Scott, 1950) and critical volume ratios (Peng, 2010). During the course of regressing data as described in Sections 3.1 and 3.2, it was found that best-fit q ratios are similar to critical volume ratios, but smaller than liquid volume ratios (Fig. 1). Thus, it is recommended that critical volumes be substituted for effective volumes in the MVL equations (the appropriate ratios are obtained when this done). Note, however, that caution should be exercised if the critical volumes of two components differ by more than a factor of ~3, or if one of the components is polar (e.g., Poling et al., 2001).

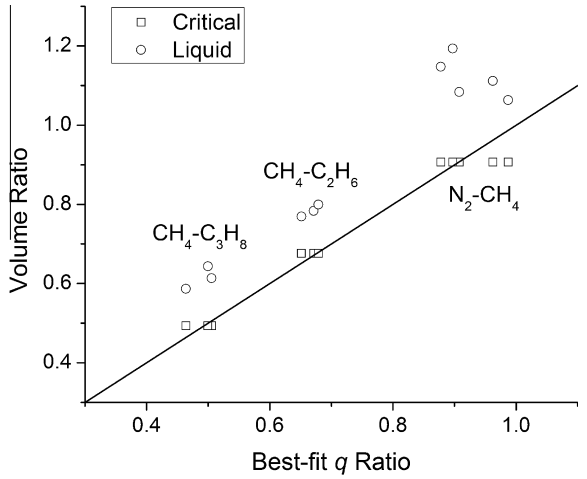

Fig. 1. Comparison of best-fit q ratios to critical and liquid volume ratios. The line designates a 1:1 correspondence. Best-fit q ratios were obtained from regressions of vapor–liquid equilibrium data along isotherms, and each point represents an isotherm. Only binaries involving CH_4 are shown because data for the other binaries in Table 1 do not cover sufficient compositional space for accurate determination of best-fit q ratios.

2.2. Solid–liquid equilibrium

Solid–liquid equilibrium can be represented by equating the fugacities of the solute k in the solid and liquid phases, that is

$$(\gamma_k x_k f_k^\circ)^{\mathrm{sol}} = (\gamma_k x_k f_k^\circ)^{\mathrm{liq}}, \quad (8)$$

which can be used to calculate the solubilities of solids in liquids on Titan. A common simplification is to assume that the solid of interest is pure (e.g., Preston and Prausnitz, 1970), so that both γ_k^{sol} and x_k^{sol} can be set to unity. This does not mean that solids must occur as pure deposits on Titan; instead, the requirement is purity on the scale of crystals. Of course, nothing is presently known about the nature of solids on Titan at this scale, and it is doubtful that such information will be available soon. On the other hand, it is arguable that solid solution formation may be inhibited on Titan owing to low surface temperatures, which will make entropically-driven mixing in crystal lattices less favorable. As a starting point, the modeling reported here assumes that solids on Titan's surface are pure phases.

Equilibrium calculations require standard state fugacities of solids and supercooled liquids, and we focus on those of C_2H_2 in this study. Fugacities are assumed to be equal to their respective vapor pressures, which provides a close approximation at temperatures below the triple point where pressures are low (<1 bar). Vapor pressures of solid C_2H_2 were taken from Tickner and Lossing (1951) and Ambrose (1956), and are represented by

$$\log(p_{C_2H_2},\ \mathrm{bar}) = 11.977\text{–}1333.01 \times T^{-1} - 0.9399 \times \ln(T), \quad (9)$$

which may be used between ~90 and 192 K (Fig. 2). Close agreement between Eq. (9) and data from Stull (1947) was also observed, but vapor pressures reported by Bourbo (1943) are up to two times larger than those from Eq. (9).

What would be the vapor pressure of liquid C_2H_2 if it could exist as a supercooled liquid? This question can be addressed using the Ambrose–Walton corresponding-states method (Poling et al., 2001). This correlation relates vapor pressures of fluids to critical properties, and gives accurate values for nonpolar fluids. Critical properties of C_2H_2 were taken from Ambrose and Townsend (1964). As shown in Fig. 2, the correlation reproduces experimental vapor pressures of liquid C_2H_2 to within ~0.3% between the triple (193 K) and critical (308 K) points. Vapor pressures of liquid C_3H_8 from the correlation were compared with those

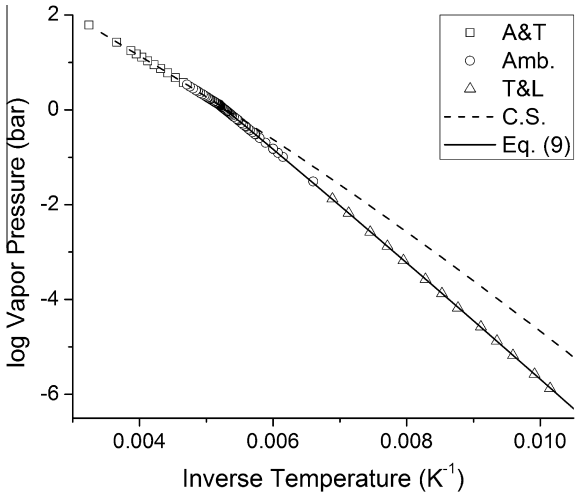

Fig. 2. Comparison of calculated and experimental vapor pressures of C_2H_2 as functions of inverse temperature. The dashed curve corresponds to vapor pressures of liquid C_2H_2 from the Ambrose–Walton corresponding-states (C.S.) method, and the curve extends into the supercooled region. The solid curve designates vapor pressures of solid C_2H_2 from Eq. (9). The curves intersect at the triple point (192.6 K, 1.282 bar; Ambrose, 1956). Symbols represent vapor pressures from experiments. Abbreviations: A&T, Ambrose and Townsend (1964); Amb., Ambrose (1956); T&L, Tickner and Lossing (1951).

from REFPROP to determine whether the correlation is also reliable at lower temperatures. Results agreed to within ~3% at temperatures from 86–370 K (C_3H_8 was chosen as a test substance because it is a well-characterized nonpolar compound with a wide temperature range of liquidity).

The solubility of a solid in a liquid depends on the ratio of standard state fugacities (equivalent to the equilibrium constant; Anderson, 2005), rather than on individual fugacity values. In the case of C_2H_2, the fugacity ratio (from ~60–192 K) can be represented by

$$\log\left(\frac{f^{\mathrm{sol}}}{f^{\mathrm{liq}}}\right)^{\circ}_{C_2H_2} = 1.6463\text{–}371.46 \times T^{-1} + 10,548 \times T^{-2}, \quad (10)$$

which was fit to numerical data generated from Eq. (9), and to results (90–192 K) from the Ambrose–Walton corresponding-states equation in Poling et al. (2001). Graphical analysis (not shown) revealed that the derivative of the logarithm of the fugacity ratio with respect to inverse temperature is approximately linear, permitting a quadratic extrapolation down to 60 K. Eq. (10) has an estimated uncertainty of ~0.5 log units.

It should be noted that there is an alternative method of calculating the standard state fugacity ratio. The key equation is (Preston and Prausnitz, 1970)

$$\ln\left(\frac{f^{\mathrm{sol}}}{f^{\mathrm{liq}}}\right)^{\circ}_{C_2H_2} = \frac{\Delta S^{\circ}_{\mathrm{fus}}}{R}\left(1-\frac{T_t}{T}\right) + \frac{\Delta C^{\circ}_p}{R}\left(\frac{T_t}{T}-1\right) - \frac{\Delta C^{\circ}_p}{R}\ln\left(\frac{T_t}{T}\right), \quad (11)$$

where ΔS°_{fus} stands for the entropy of fusion at the triple-point temperature (T_t), and ΔC°_p indicates the difference in isobaric heat capacity between the liquid and solid forms of the solute at T_t. The entropy of fusion of C_2H_2 is ~20 J mol^{-1} K^{-1} (Preston and Prausnitz, 1970; Miskiewicz et al., 1976), but we were unable to find heat capacities for solid or liquid C_2H_2 in the literature. Nevertheless, Eq. (11) can be evaluated if it is assumed that the last two terms in the equation cancel out (Preston and Prausnitz, 1970). This simplified form of Eq. (11) gives standard state fugacity ratios that are consistent with those from Eq. (10) to within ~20% between 90 and 193 K, but the equations give results that diverge rapidly below 90 K, presumably because we neglected the heat capacity terms in Eq. (11), which assume greater quantitative significance at lower temperatures. Therefore, for C_2H_2, Eq. (10) is preferable to the simplified form of Eq. (11) because the former equation is based on a less severe assumption (corresponding-states) than that for the latter equation (no heat capacity terms). It should be emphasized, however, that the situation may be the opposite for other compounds relevant to Titan, with thermal data being more plentiful or reliable, and vapor pressure data being less available or reliable. In those cases (which may be common), Eq. (11) would be preferred.

3. REGRESSION OF BINARY DATA

Binary phase equilibrium data that can be used to parameterize the MVL model and other geochemical models at Titan surface temperatures (~90–95 K) are summarized in Table 1. Vapor–liquid equilibrium (VLE) data consist of measurements of liquid-phase composition, total pressure, and temperature (the composition of the vapor phase is given in some cases). Solid–liquid equilibrium (SLE) data correspond to solid solubility as a function of temperature. Compositions of immiscible liquids, total pressures, and temperatures are reported in studies of liquid–liquid equilibrium (LLE). In this study, LLE were not considered because it is unlikely that LLE exist on Titan (Thompson, 1985), because the partial pressure of N_2 at Titan's surface (~1.4 bar) is too low to induce phase splitting. Extrapolation of separation pressures for the N_2–C_2H_6 system indicates that two liquid phases should form only if $p_{N_2} > 3.8$ bar at 91 K (Gasem et al., 1981). The N_2–C_3H_8 binary requires similar pressures for phase separation (Schindler et al., 1966). In contrast, N_2 and CH_4 are miscible (see below). The MVL model should not be used whenever LLE are suspected (e.g., C_2H_6- or C_3H_8-rich systems containing N_2 near the saturation pressure of liquid N_2).

Binary VLE data were regressed using Barker's method (Barker, 1953), which is a standard technique for determining parameters in Raoultian activity coefficient models. Least squares fitting yielded parameters in Eqs. (6) and (7) that minimize differences between calculated and experimental total pressures. The fitting procedure was iterative. Because best-fit q ratios were found to be similar to critical volume ratios (Fig. 1), q ratios in Eqs. (6) and (7) were replaced with the respective critical volume ratio (Table 2). This reduces the MVL model to a one-parameter form,

Table 1
Experimental phase equilibrium data for some binary mixtures that are relevant to cryogenic fluvial geochemistry on Titan. Abbreviations: VLE, vapor–liquid equilibrium; SLE, solid–liquid equilibrium; LLE, liquid–liquid equilibrium.

Reference	Type of data	Temperature range (K)	Used in this work?
CH_4–C_2H_6			
Gomes de Azevedo and Calado (1989)	VLE	90.69–103.99	Yes
Miller and Staveley (1976)	VLE	115.77	Yes
Wilson (1975)	VLE	110.93	No
CH_4–C_3H_8			
Calado et al. (1974)	VLE	115.77–134.83	Yes
Cheung and Wang (1964)	VLE	91.7–128.4	No
Cutler and Morrison (1965)	VLE	90–110	No
Poon and Lu (1974)	VLE	114.1–122.2	No
Stoeckli and Staveley (1970)	VLE	90.68	Yes
Wilson (1975)	VLE	110.93	No
C_2H_6–C_3H_8			
Djordjevich and Budenholzer (1970)	VLE	127.59–255.37	Yes (127.59–172.04 K)
N_2–CH_4			
Cheung and Wang (1964)	VLE	91.6–124.1	No
Fuks and Bellemans (1967)	VLE	84.15–90.84	No
Gabis (1991)	VLE	84.84–94.04	Yes
McClure et al. (1976)	VLE	90.68	Yes
Omar et al. (1962)	VLE, SLE	~58–98	No
Parrish and Hiza (1974)	VLE	95–120	Yes (95–110 K)
Sprow and Prausnitz (1966)	VLE	90.67	No
Stryjek et al. (1974)	VLE	113.71–183.15	No
Wilson (1975)	VLE	110.93	No
N_2–C_2H_6			
Cheung and Wang (1964)	VLE	92.8	No
Ellington et al. (1959)	VLE, LLE	99.82–299.82	Yes (99.82–110.93)
Guedes et al. (2002)	VLE, LLE	90.69	No
Kremer and Knapp (1983)	VLE, LLE	120–133.15	Yes (120 K)
Llave et al. (1985)	VLE, LLE	118–132.38	Yes (118–120 K)
Szczepaniec-Cieciak et al. (1980)	SLE	69.5–85.5	Yes
Wilson (1975)	VLE, LLE	110.93	Yes
Yu et al. (1969)	VLE, LLE	113.71–133.26	Yes (113.71–119.26 K)
N_2–C_3H_8			
Cheung and Wang (1964)	VLE	91.9–128.4	Yes (91.9–110.2 K)
Houssin-Agbomson et al. (2010)	VLE	109.98–125.63	Yes (109.98–119.75 K)
Kremer and Knapp (1983)	VLE, LLE	120–127	Yes (120 K)
Llave et al. (1985)	VLE, LLE	117–126.62	No
Poon and Lu (1974)	VLE	114.1–122.2	No
Schindler et al. (1966)	VLE, LLE	103.15–353.15	Yes (103.15 K)
Szczepaniec-Cieciak et al. (1980)	SLE	64.8–101	Yes (64.8–85 K)
C_2H_2–CH_4			
Neumann and Mann (1969)	SLE	93.3–143.1	Yes
C_2H_2–N_2			
Fedorova (1940)	SLE	65–95	Yes
Ishkin and Burbo (1939)	SLE	77.4	Yes

which brings the benefits discussed in Section 2.1; and does not introduce significant inaccuracies (see below). Binary SLE data were regressed by applying least squares fitting to reported solubilities. While all of the datasets listed in Table 1 were analyzed, only a subset of the data was used in the final regressions. Decisions were made by examining trends in derived values of ω_{12}, which vary smoothly with temperature for mutually consistent data. The recommendations of Hiza et al. (1979), Miller et al. (1980), and Kidnay et al. (1985) were also given preference. Note that data not used in the final regressions are not necessarily "bad", but they are less consistent than other data.

Activity coefficients depend on the temperature, pressure, and composition of the phase of interest. The MVL model accounts for the composition dependence via mole fraction terms. The temperature dependence is represented by specifying interaction energies as $\omega_{ij} = \omega_0 + \omega_1 T + \omega_2 T \times \ln(T)$, where subscripted parameters denote constants

Table 2
Physical and thermodynamic properties of some compounds on Titan ($P_{ref} = 1.467$ bar, $T_{ref} = 90.6941$ K).

Compound	Critical volume ($cm^3\ mol^{-1}$)	Volume at P_{ref} and T_{ref} ($cm^3\ mol^{-1}$)	Enthalpy of vaporization at T_{ref} ($J\ mol^{-1}$)	Fugacity at P_{ref} and T_{ref} (bar)	ΔG_f° ($kJ\ mol^{-1}$)
CH_4	98.6291[a]	35.5342 (liq.)[a]	8731[a]	0.1168 (liq.)[a]	−64.744 (gas)[h] −66.363 (liq.)[i]
C_2H_6	145.8388[a]	46.1732 (liq.)[a]	17,873[a]	1.255×10^{-5} (liq.)[a]	−63.827 (gas)[j] −72.337 (liq.)[i]
C_3H_8	200[a]	60.5882 (liq.)[a]	24,587[a]	1.261×10^{-8} (liq.)[a]	−73.394 (gas)[j] −87.11 (liq.)[i]
N_2	89.4142[a]	37.8343 (liq.)[a]	5023[a]	3.408 (liq.)[a]	0 (gas)[h] 0.9246 (liq.)[i]
C_2H_2	112.2[b]	35 (liq.)[c] 33.4 (sol.)[d]	20,648[e]	1.63×10^{-6} (liq.)[f] 1.1×10^{-7} (sol.)[g]	221.584 (gas)[h] 211.535 (liq.)[i] 209.502 (sol.)[i]

[a] Lemmon et al. (2010).
[b] Poling et al. (2001).
[c] Estimated by scaling a volume near the triple point (McIntosh, 1907) with the Rackett equation (Poling et al., 2001).
[d] Lunine et al. (1983).
[e] Estimated by scaling the enthalpy of vaporization at the triple point (Ambrose, 1956) with the Watson relation (Poling et al., 2001).
[f] Estimated using the Ambrose–Walton corresponding-states method (Poling et al., 2001).
[g] Computed using Eq. (9).
[h] Chase (1998).
[i] Derived from the standard Gibbs energy of formation (ΔG_f°) of the gas from the elements, and from the fugacity of the condensed phase.
[j] Chao et al. (1973).

that are determined by regressing experimental data at different temperatures. In some cases, the data do not warrant a value for ω_2. Interaction energies are parameterized over certain temperature intervals, and extrapolations are governed by *caveat emptor*. We did not account for the effects of pressure on activity coefficients because pressure effects should be negligible, except at high pressures (>100 bar or >10 km depth on Titan). Binary solutions of nonpolar compounds of interest have small excess volumes of mixing (generally between 0 and $-2\ cm^3\ mol^{-1}$; e.g., Hiza et al., 1979; Miller et al., 1980; Kidnay et al., 1985), which means that mixing is nearly ideal with respect to volume. This makes activity coefficients weak functions of pressure. Exceptions are systems close to the critical point of a component. For this reason, data at temperatures >120 K for systems with N_2 (critical temperature, 126.19 K) were not included in the regressions.

3.1. Vapor–liquid equilibria of hydrocarbon mixtures

Comparisons between model results and experimental data make it possible to assess the strengths and weaknesses of the MVL model. Results for VLE regressions of hydrocarbon systems are shown in Fig. 3, and the corresponding interaction energies are given in Table 3. These parameters can be used to perform calculations for arbitrary compositions.

The MVL model accurately reproduces the experimental data. The model is most accurate for the CH_4–C_2H_6 binary, for which computed pressures agree with measured values

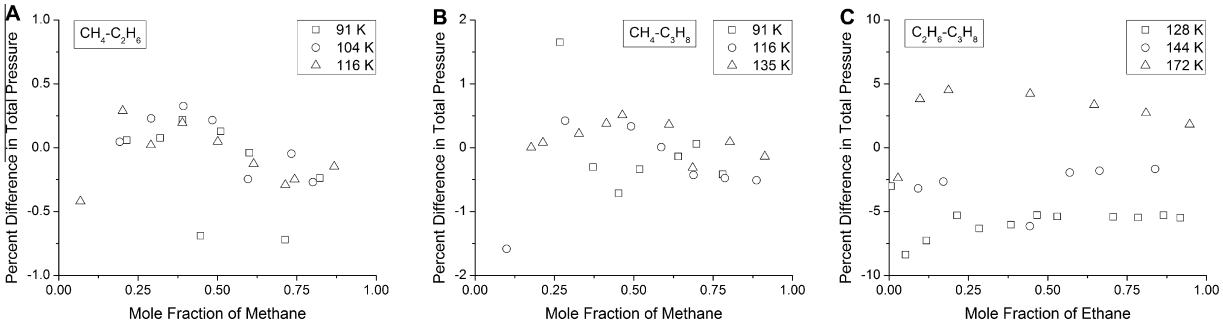

Fig. 3. Comparison of total pressures from the modified van Laar model to total pressures from experiments for the (A) CH_4–C_2H_6, (B) CH_4–C_3H_8, and (C) C_2H_6–C_3H_8 binaries. Symbols represent percent differences between computed and measured pressures (i.e., residuals), as a function of liquid-phase composition and temperature. The experimental data in (A) are from Gomes de Azevedo and Calado (1989) [91 K, 104 K], and Miller and Staveley (1976) [116 K]. In (B), the experimental data are from Stoeckli and Staveley (1970) [91 K], and Calado et al. (1974) [116 K, 135 K]. All of the experimental data in (C) are from Djordjevich and Budenholzer (1970). Note the differing scales and abscissa of the plots.

Table 3
Interaction energy parameters for the modified van Laar model ($T_{ref} = 90.6941$ K).

System	$\omega_{ij} = \omega_0 + \omega_1 T + \omega_2 T \times \ln(T)$			Temperature range (K)	ω_{ij} at T_{ref} (J mol^{-1})
	ω_0	ω_1	ω_2		
CH_4–C_2H_6	1366	−36.68	7.143	90.69–115.77	959
CH_4–C_3H_8	2412	−58.11	11.279	90.68–134.83	1753
C_2H_6–C_3H_8[a]	0	0	0	127.59–172.04	~0
N_2–CH_4	2443	−75.16	14	84.84–110	1350
N_2–C_2H_6	1797	27.79	0	69.5–120	4317
N_2–C_3H_8	2099	50.05	0	64.8–120	6638
C_2H_2–CH_4	14,940	−50.34	0	93.3–143.1	~10,374
C_2H_2–C_2H_6	2416[b]	0	0	90.6941	~2416
C_2H_2–C_3H_8	3429[b]	0	0	90.6941	~3429
C_2H_2–N_2	6886	51.92	0	65–95	11,595
CH_4–C_2H_6–N_2	2604	0	0	95	~2604

[a] This system is approximately ideal at low temperatures (see Fig. 3C).
[b] Estimated using the correlation for C_2H_2 in Fig. 6.

to within ~1% (Fig. 3A). The discrepancies for the CH_4–C_3H_8 binary are only slightly larger (Fig. 3B). In both of these systems, the residuals in total pressure exhibit either no or weak trends with composition or temperature (Fig. 3A and B), providing additional evidence that the model provides a close representation of the experimental data.

The C_2H_6–C_3H_8 binary was treated differently, as it was assumed to be an ideal solution (i.e., $\omega_{ij} = 0$). An initial attempt was made to derive interaction energies by regressing VLE data. However, derived values were inconsistent, showing no apparent trend with temperature. It appears that the uncertainties in the experimental data are larger than the small deviations from ideality of this system. We tested this idea by assuming ideal behavior in Fig. 3C. It can be seen that the ideal assumption yields total pressures that are within ~5–10% of the measured values. Djordjevich and Budenholzer (1970) reported that the experimental pressures have errors of up to 4%, and the composition measurements have an uncertainty of 3 mol%. Overall, the C_2H_6–C_3H_8 binary deviates from ideality by a small amount (~5%), which means that the ideal assumption is sufficient for applications of interest to Titan.

3.2. Vapor–liquid equilibria of systems with N_2

The MVL model reproduces the experimental data for the N_2–CH_4, N_2–C_2H_6, and N_2–C_3H_8 binaries with respectable accuracy, although there are some issues (Fig. 4). The model is most accurate for the N_2–CH_4 binary, for which computed pressures agree with measured values to within ~2% (Fig. 4A). The discrepancies become larger as the alkane becomes larger; deviations in total pressure of ~5–10% characterize N_2–C_2H_6 (Fig. 4B), while N_2–C_3H_8 features larger deviations of ~10–20% (Fig. 4C). However, the N_2–C_3H_8 binary is of lesser importance because C_3H_8 is probably much less abundant than C_2H_6 on Titan (see Section 5.1). For N_2–C_2H_6 and N_2–C_3H_8, the MVL model gives less accurate results when the mole fraction of N_2 in the liquid phase is small (Fig. 4B and C). Trends in the residuals imply that the MVL model does not capture all of the complexities of these systems. This is the cost of making a simple model with general applicability, although the errors are relatively small.

We also compared computed and measured solubilities of solid C_2H_6 and C_3H_8 in liquid N_2 (not shown), and found that calculated values agree with data reported by Szczepaniec-Cieciak et al. (1980) to within ~15%. This suggests that the interaction energies in Table 3 are not just fitting parameters, but they may have a physical basis given that they are consistent with both VLE and SLE (the common feature is the liquid solution).

3.3. Solubility of solid C_2H_2 in liquid hydrocarbons and N_2

The MVL model can also be used to accurately represent liquid-phase non-idealities in SLE. Computed solubilities of solid C_2H_2 in liquid CH_4 are within ~10% of the experimental values (Fig. 5A). A close fit was also obtained for C_2H_2 in N_2 (Fig. 5B). The model parameters that were used to generate the curves in Fig. 5 can be found in Eq. (10), and Tables 2 and 3.

SLE data could not be found for the C_2H_2–C_2H_6 and C_2H_2–C_3H_8 binaries at relevant temperatures, so a new correlation was used to estimate the interaction energies at 90.6941 K (the triple-point temperature of CH_4). We discovered that regressed interaction energies follow linear trends with differences in enthalpies of vaporization between the binary components (Fig. 6). There are linear relationships for N_2 and CH_4 with the C_1–C_3 alkanes, and the lines go through the origin (coefficient of determination, $R^2 > 0.99$). This simple behavior suggests that the interaction energies for C_2H_2–C_2H_6 and C_2H_2–C_3H_8 can be estimated using the dashed line (C_2H_2-alkane correlation) in Fig. 6, together with enthalpies of vaporization from Table 2. The estimated interaction energies are given in Table 3.

The correlations shown in Fig. 6 deserve discussion. First, we adopt a temperature of 90.6941 K, which is the triple-point temperature of CH_4 (Setzmann and Wagner, 1991); and advocate that this temperature be adopted as the reference temperature for studies of fluvial geochemistry

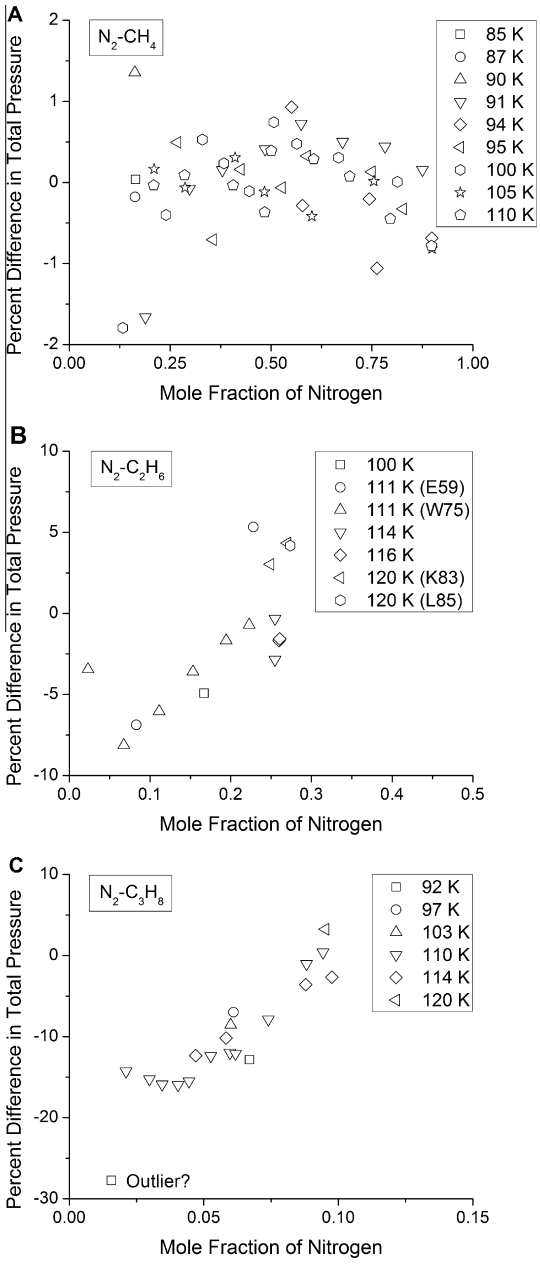

Fig. 4. Comparison of total pressures from the modified van Laar model to total pressures from experiments for the (A) N_2–CH_4, (B) N_2–C_2H_6, and (C) N_2–C_3H_8 binaries. Symbols represent percent differences between computed and measured pressures (i.e., residuals), as a function of liquid-phase composition and temperature. The experimental data in (A) are from Gabis (1991) [85–90 K, 94 K], McClure et al. (1976) [91 K], and Parrish and Hiza (1974) [95–110 K]. In (B), the experimental data are from Ellington et al. (1959) [100 K, 111 K (E59)], Wilson (1975) [111 K (W75)], Yu et al. (1969) [114–116 K], Kremer and Knapp (1983) [120 K (K83)], and Llave et al. (1985) [120 K (L85)]. The experimental data in (C) are from Cheung and Wang (1964) [92–97 K], Schindler et al. (1966) [103 K], Houssin-Agbomson et al. (2010) [110–114 K], and Kremer and Knapp (1983) [120 K]. The data in (B) and (C) do not cover the entire compositional range because there are miscibility gaps (i.e., where intermediate compositions are less stable than two liquid phases). Note the differing scales of the plots.

on Titan by the geochemical community. There are two reasons for this: (1) surface temperatures on Titan are within a few Kelvin of the recommended value (Fulchignoni et al., 2005; Jennings et al., 2009), and (2) the recommended temperature is easily achieved in the laboratory using the solid–liquid equilibrium of CH_4 as a cryostat. The situation is analogous to terrestrial geochemistry, where 298.15 K is adopted as the reference temperature because it is both relevant and convenient (e.g., Garrels and Christ, 1965; Anderson, 2005). Second, it makes intuitive sense that interaction energies correlate positively with differences in enthalpies of vaporization. The enthalpy of vaporization provides a measure of the strength of intermolecular forces in a liquid. A larger difference in enthalpies of vaporization means that the interactions between molecules in two liquids are less similar, so the mixture should be less ideal and have a larger value of ω_{ij}. This may also explain why the lines in Fig. 6 pass through the origin. Third, there is the question of uncertainties, which is difficult to address. However, numerical tests indicate that if C_2H_2 follows a linear correlation but the slope in Fig. 6 is in error by say 10%, predicted solubilities of solid C_2H_2 in liquid C_2H_6 or C_3H_8 would be uncertain by ~20%. On the other hand, the predicted solubility could be uncertain by a factor of at least several if linear behavior does not hold. Finally, the simplicity of the correlations in Fig. 6 suggests that it may be possible to develop completely predictive correlations for systems that have not been experimentally characterized, such as C_2N_2(cyanogen)–C_2H_6, if the slope of lines in Fig. 6 can be estimated using only pure-component properties (e.g., critical temperature, acentric factor, polarizability, second virial coefficient).

4. COMPARISONS BETWEEN MODELS OF TERNARY SYSTEMS

4.1. Vapor–liquid equilibria of CH_4–C_2H_6–N_2

Liquids on Titan should be multicomponent mixtures (Lunine et al., 1983; Raulin, 1987; Cordier et al., 2009). Thus, it is vital to test the MVL model using experimental data for systems containing more than two components. However, experimental phase equilibrium data for ternary systems at conditions relevant to Titan's surface are scarce. Almost all of the available data are for temperatures that are too high (e.g., Chang and Lu, 1967; Yu et al., 1969; Wichterle and Kobayashi, 1972; Poon and Lu, 1974; Llave et al., 1987). The notable exception is Gabis (1991) who obtained data at 95 K for the CH_4–C_2H_6–N_2 system, which is regarded as the most important ternary on Titan (Lunine et al., 1983) and therefore represents a crucial test for the MVL model. Ternary VLE data from Gabis (1991) are given in Supplementary Table 1, as they are useful and from a rare, unpublished source. Gabis (1991) performed experiments inside a vapor recirculation cell, where vapor is pumped through liquid to facilitate equilibrium. This type of apparatus is commonly used in studies of low-temperature VLE. Pressure was measured using a Bourdon gauge (±0.01 bar), temperature was measured using a resistance thermometer (±0.2 K), and composition was determined

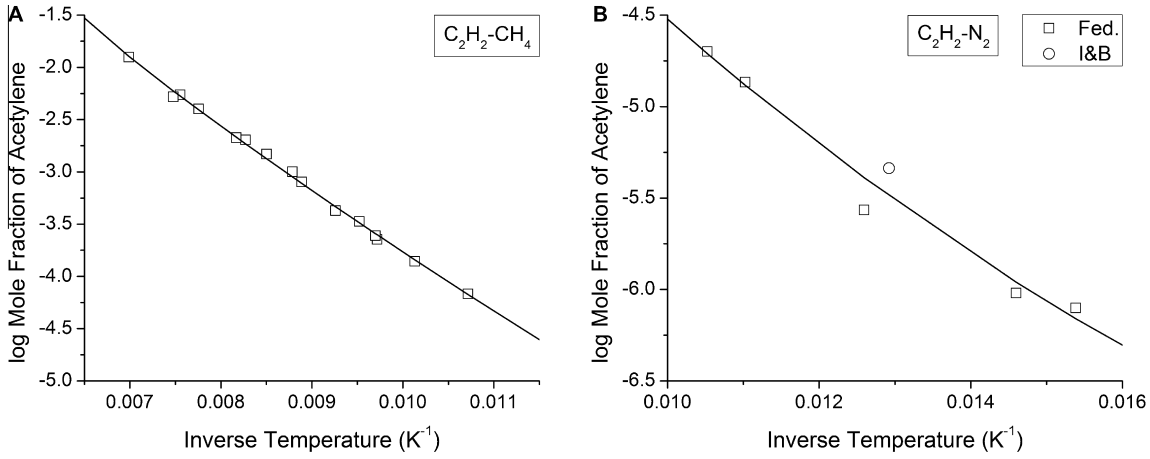

Fig. 5. Solubility of solid C_2H_2 in liquid (A) CH_4 and (B) N_2, as a function of inverse temperature at the saturation pressure of the solvent. In (A), symbols denote experimental data from Neumann and Mann (1969); and symbols denote experimental data from Fedorova (1940) [abbr. Fed.] and Ishkin and Burbo (1939) [abbr. I&B] in (B). The curves correspond to predicted solubilities from the modified van Laar model. Note the differing scales of the plots.

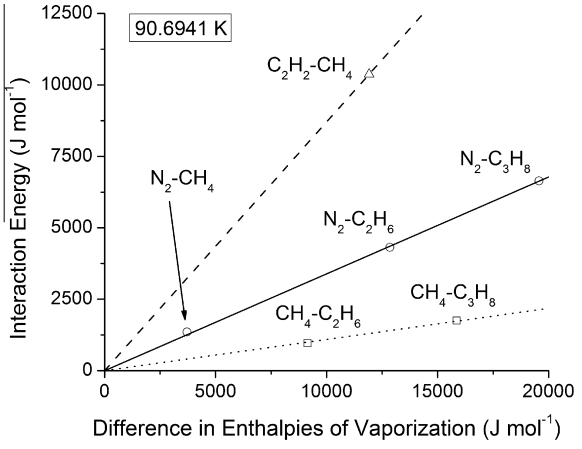

Fig. 6. Linear correlations between binary interaction energies and differences in enthalpies of vaporization at 90.6941 K. Symbols correspond to absolute differences in enthalpies of vaporization from Table 2, and interaction energies for binary systems from Table 3. Lines represent correlations for species in liquid alkanes, converging at the origin; and the slopes of the lines for CH_4, N_2, and C_2H_2 are 0.1091, 0.3389, and 0.8705, respectively.

using gas chromatography (±0.003 mol fraction). It is notable that VLE data for N_2–CH_4 from Gabis (1991) are consistent with N_2–CH_4 data from McClure et al. (1976) and Parrish and Hiza (1974) to within a few percent (Fig. 4A). CH_4–C_2H_6–N_2 data from Gabis (1991) are used in the present study to determine how well the MVL model and other models extrapolate to the ternary system.

Various models of VLE in the CH_4–C_2H_6–N_2 ternary at 95 K are compared in Fig. 7. Raoult's law provides the simplest description by assuming that the mixture is ideal. It can be seen that Raoult's law is the least accurate model (Fig. 7A), and always underestimates the total pressure. In other words, N_2 gas is predicted to be too soluble in the liquid phase. Raoult's law deviates more in C_2H_6-rich systems. Evidently, interactions between N_2 and C_2H_6 molecules exhibit large departures from ideal behavior. Raoult's law is an insufficient model for this ternary, and provides crude approximations at best.

The model of Heintz and Bich (2009) was developed with Titan in mind. Activity coefficients are calculated with a one-parameter Margules equation. Results from the Heintz and Bich (2009) model resemble those from Raoult's law, but the Heintz and Bich (2009) model provides minor improvements over Raoult's law by predicting slightly higher pressures (Fig. 7A). However, the model also gives results that are significantly inaccurate for C_2H_6-rich systems. This may be surprising because a one-parameter Margules equation is expected to provide greater improvement over Raoult's law. It is unclear how Heintz and Bich (2009) determined the Margules parameter for N_2–C_2H_6, as none of the references they cite contain data on VLE for the N_2–C_2H_6 binary.

The model of Preston and Prausnitz (1970) is based on Scatchard–Hildebrand regular solution theory, with one empirical parameter per binary. This model is popular in the Titan literature (e.g., Dubouloz et al., 1989; Cordier et al., 2009), so its accuracy should be assessed. As shown in Fig. 7A, the model provides a close representation of VLE for CH_4-rich systems (to within ~15%), but the model predicts total pressures that are too high by about a factor of two for systems enriched in C_2H_6. There is a systematic trend in the results (Fig. 7A), which suggests that there is a deficiency in the representation of the N_2–C_2H_6 endmember; N_2 gas should be more soluble in liquid C_2H_6. It appears that the binary parameter for N_2–C_2H_6 should be more negative than the value given by Preston and Prausnitz (1970). It is recommended that users of this model re-evaluate the parameter using references in Table 1. Cordier et al. (2012) attempted to estimate uncertainties in their regular-solution calculations by performing Monte Carlo simulations, but the direct approach of making comparisons between predictions from the model and experimental phase equilibrium data would be more informative.

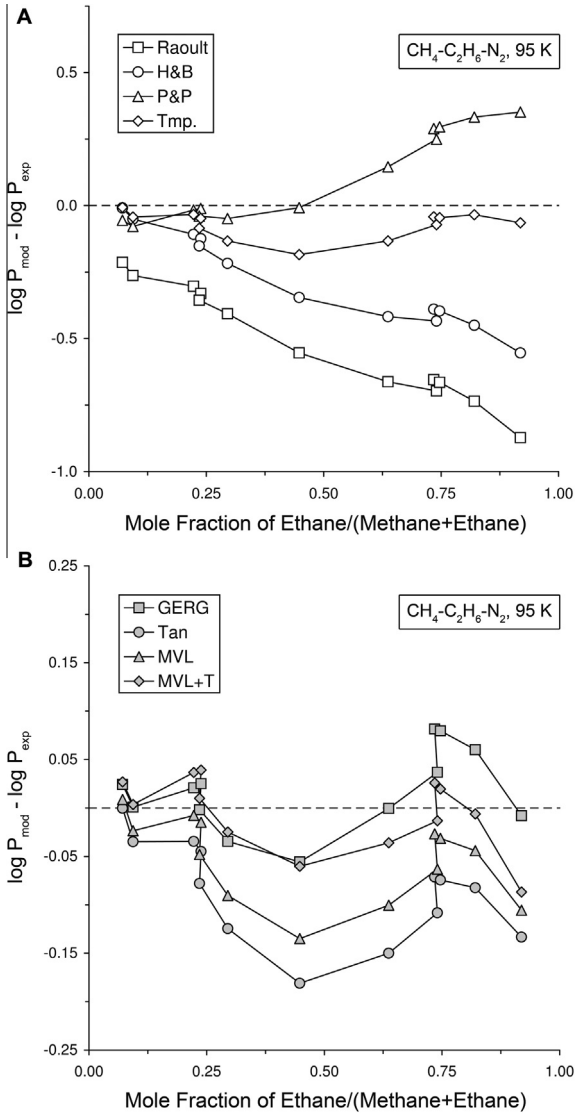

Fig. 7. (A) Comparisons between some models of the CH_4–C_2H_6–N_2 ternary at 95 K, and (B) a zoomed in perspective of the results from a few other models. Symbols show differences between common logarithms of total pressures from models and experiments (Supplementary Table 1), as a function of the relative amounts of CH_4 and C_2H_6 in the liquid. Points are connected by lines to highlight trends. The dashed horizontal line corresponds to perfect agreement between model and experiment. Raoult refers to Raoult's law, and GERG refers to the GERG model (Kunz et al., 2007; Kunz and Wagner, 2012). Abbreviations: H&B, Heintz and Bich (2009); P&P, Preston and Prausnitz (1970); Tmp., Thompson (1985); Tan, Tan et al. (2013); MVL, modified van Laar (Eq. (3)); MVL+T, modified van Laar with a ternary parameter (Eq. (12)).

The model of Thompson (1985) has also been used in studies of Titan (e.g., Raulin, 1987; McKay et al., 1993). Activity coefficients are computed using one-parameter Margules equations, with empirically determined exponents of one or two in the activity coefficient equations. Thus, the Thompson (1985) model was formulated similarly to that of Heintz and Bich (2009), but the latter model uses a fixed exponent of two for binaries. Thompson's model is fairly consistent with the experimental ternary data, and it is considerably more accurate than the Heintz and Bich (2009) model (Fig. 7A). The largest discrepancies in total pressure (~20–30%) occur where CH_4 and C_2H_6 are approximately equimolar, suggesting that three-body interactions are largely responsible for the discrepancies (the model features binary terms only). A key concern is that the Thompson (1985) model is not thermodynamically consistent, as it does not satisfy the Gibbs–Duhem equation. Modifying activity coefficient equations empirically led to this inconsistency. This problem can be prevented if empirical modifications are made to the equation for the excess Gibbs energy of mixing instead (Prausnitz et al., 1999). Thompson recognized this in later works on the N_2–CH_4 binary (Thompson et al., 1990, 1992), but he did not revisit more complex mixtures.

The Groupe Europeen de Recherches Gazieres (GERG; Kunz et al., 2007; Kunz and Wagner, 2012) model is the most sophisticated model that was tested. We acquired the model as part of the NIST REFPROP software package (Lemmon et al., 2010). The model was developed for technical applications in the natural gas industry, and uses equations of state for fluids that are explicit in the Helmholtz energy. The equations of state are accurate over wide ranges of density, temperature, and composition. Thermodynamic properties of mixtures are computed using departure functions that were fit to binary data. These functions account for non-ideal behavior, and they contain four empirical parameters per binary system. The GERG model reproduces the experimental pressures to within ~15%, with deviations that are weakly systematic at most (Fig. 7B). In terms of accuracy, the GERG model is impressive. The version in REFPROP is also easy-to-use, featuring a graphical user interface. However, the GERG model has certain disadvantages with respect to Titan applications. Its complex mathematical structure (see Kunz et al., 2007; Kunz and Wagner, 2012) makes the model difficult to modify or expand, and deriving parameters for the model requires complex, non-linear regression algorithms. Another shortcoming is that the user-friendly version of the model in REFPROP cannot be applied to equilibria involving solids, rendering it inapplicable to solving many geochemical problems on Titan. This is not an insurmountable obstacle, but adaptation of the model to SLE would require additional research to maintain internal consistency of the thermodynamic data.

The perturbed-chain statistical associating fluid theory of Tan et al. (2013) deserves discussion because it is the most recent phase equilibrium model developed for application to Titan. In this model, non-spherical molecules are viewed as chains that are composed of spherical segments. The nine-component model has a theoretical basis in molecular perturbation theory, can be extended to multicomponent mixtures using one empirical parameter per binary system, and accurately reproduces VLE over wide ranges of density, temperature, and composition. These favorable attributes are counteracted by drawbacks that are identical to those of the GERG model: the Tan et al. (2013) model cannot be used to compute the solubility of solids in liquids, although the authors state that they are addressing this; and

the model is unnecessarily complex for geochemical applications of present interest. Unlike the GERG model, a user-friendly version of the Tan et al. (2013) model is not available. The Tan et al. (2013) model is also less accurate than the GERG model with respect to the CH_4–C_2H_6–N_2 ternary at 95 K (Fig. 7B). The largest discrepancies in total pressure are ~20–30%, which is similar to the performance of the Thompson (1985) model. It appears that the added complexity of the Tan et al. (2013) model does not necessarily translate into more accurate results. Nevertheless, this model is probably sufficiently accurate for application to Titan, as demonstrated by their compelling interpretation of the Huygens GC–MS data.

The MVL model ranks second place – it is slightly (i.e., a few percent) more accurate than the models of Thompson (1985) and Tan et al. (2013), but slightly less accurate than the GERG model (Fig. 7B). The overall agreement with the experimental data is encouraging (within ~20%), and suggests that Eq. (3) may provide sufficient representations of non-idealities in other multicomponent systems of interest. The deviations in the MVL model are greatest where CH_4 and C_2H_6 are about equally abundant. As mentioned above, this appears to be a ternary effect, which should be strongest at the midpoint in Fig. 7B. This effect can be accounted for by adding a ternary term to the model, leading to the general equation for activity coefficients from the MVL model given by (see Appendix A)

$$RT \times \ln(\gamma_k^{\mathrm{liq}}) = -\sum_{i=1}^{n-1}\sum_{j>i}^{n}\frac{\omega_{ij}\lambda_i\lambda_j q_k}{q_i + q_j} + \sum_{a=1}^{n-2}\sum_{b>a}^{n-1}\sum_{c>b}^{n}\frac{\omega_{abc}\delta_a\delta_b\delta_c q_k}{4(q_a + q_b + q_c)}, \quad (12)$$

where ω_{abc} represents the interaction energy for ternary a–b–c, and auxiliary function δ is expressed in terms of the effective volume fraction as $\delta_i = 1 - 2z_i$ when $i = k$, or $\delta_i = -2z_i$ when $i \neq k$. As an example, the activity coefficient of N_2 in the three-component liquid can be written as

$$\begin{aligned} RT \times \ln(\gamma_{N_2}^{\mathrm{liq}}) = {} & \frac{\omega_{N_2\text{–}CH_4}(1 - z_{N_2})z_{CH_4}q_{N_2}}{q_{N_2} + q_{CH_4}} \\ & + \frac{\omega_{N_2\text{–}C_2H_6}(1 - z_{N_2})z_{C_2H_6}q_{N_2}}{q_{N_2} + q_{C_2H_6}} \\ & - \frac{\omega_{CH_4\text{–}C_2H_6}z_{CH_4}z_{C_2H_6}q_{N_2}}{q_{CH_4} + q_{C_2H_6}} \\ & + \frac{\omega_{CH_4\text{–}C_2H_6\text{–}N_2}z_{CH_4}z_{C_2H_6}(1 - 2z_{N_2})q_{N_2}}{q_{CH_4} + q_{C_2H_6} + q_{N_2}} \end{aligned} \quad (13)$$

Applying Eq. (12) to the Gabis (1991) dataset (Supplementary Table 1) yields an interaction energy for CH_4–C_2H_6–N_2 of 2604 J mol^{-1} at 95 K. Interestingly, this value is somewhat close to the arithmetic mean of the constituent binaries (2256 J mol^{-1}). This could be a coincidence, or a hint of a predictive scheme. Additional experimental data for ternary systems will need to be obtained and regressed to determine which.

Adding a ternary term to the MVL model (i.e., MVL+T) increases the accuracy of the model by ~5–10%, as shown in Fig. 7B. Furthermore, the refined model is, on average, a few percent more accurate than the GERG model. The improvements highlight the flexible architecture of the MVL model. It was also found that computed vapor compositions compare favorably to those reported by Gabis (1991) (p_{N_2} within ~2%, p_{CH_4} within ~20%). The ternary term shifts the MVL line segment in Fig. 7B upward, with the largest shifts occurring around the CH_4–C_2H_6 midpoint. The maximum absolute deviation in total pressure is now 18% (previously 27%), and corresponds to the most C_2H_6-rich composition. This discrepancy most likely reflects deficiencies in the simplistic description of the N_2–C_2H_6 binary (see Section 3.2), but the magnitude of the discrepancy is tolerable for Titan applications at present.

Analysis of the individual terms in Eq. (13) revealed that non-ideal behavior in the CH_4–C_2H_6–N_2 system is mostly controlled by binary interactions, while forces between three different molecules fine-tune the system. Based on this finding, a hybrid of Eqs. (3) and (12) may be useful for geochemical modeling. Eq. (12) is the more general expression, and ternary terms should be included whenever high-quality experimental data exist. If such data are unavailable, ternary interaction energies in Eq. (12) may be set to zero (*à la* Eq. (3)), which may lead to errors on the order of tens of percent (Fig. 7B). When the MVL model is applied to complex mixtures on Titan, it can be imagined that some ternary terms will be evaluated, while most will need to be neglected, depending on the experimental data in hand and the desired accuracy. At present, all ternary terms in Eq. (12) must be excluded owing to the lack of ternary data, with the exception of that for CH_4–C_2H_6–N_2, whose interaction energy at 95 K can be assumed to be appropriate for nearby temperatures.

A summary of the aforementioned models is provided in Fig. 8 where it can be seen that Raoult's law, and the mod-

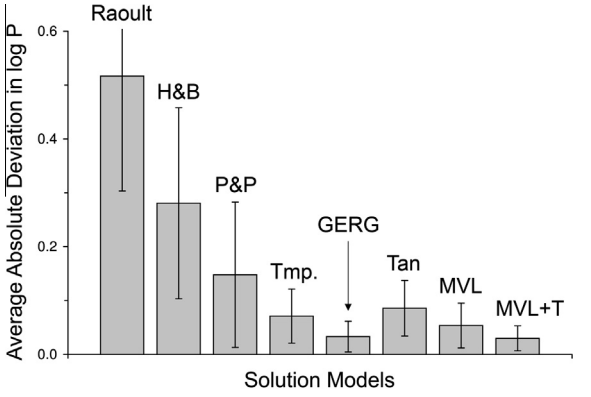

Fig. 8. Summary of models of the CH_4–C_2H_6–N_2 ternary at 95 K. Columns show averages of absolute deviations in common logarithms of total pressures from models and experiments (Supplementary Table 1). Error bars denote one standard deviation, and the error bar for Raoult's law goes off scale, but is symmetric. Raoult refers to Raoult's law, and GERG refers to the GERG model (Kunz et al., 2007; Kunz and Wagner, 2012). Abbreviations: H&B, Heintz and Bich (2009); P&P, Preston and Prausnitz (1970); Tmp., Thompson (1985); Tan, Tan et al. (2013); MVL, modified van Laar (Eq. (3)); MVL+T, modified van Laar with a ternary parameter (Eq. (12)).

els of Heintz and Bich (2009) and Preston and Prausnitz (1970) deviate most from the experimental ternary data. Therefore, these models should not be used to represent VLE involving CH_4, C_2H_6, and N_2 on Titan. Thompson's (1985) model provides adequate agreement, but is inferior to the MVL model. The latter possesses comparable simplicity but yields more accurate results than the Thompson (1985) model, and the MVL model maintains thermodynamic consistency. The GERG, Tan et al. (2013), MVL, and MVL+T models can all be used to investigate fluvial geochemistry on Titan with confidence (Fig. 8). Choosing between them depends on the specific application and personal preference. If the user is interested in VLE only (e.g., clouds) and wants user-friendly software that is relatively inexpensive (http://www.nist.gov/srd/nist23.cfm), then the GERG model would be an excellent choice. The MVL or MVL+T model would be preferred if the application of interest involves the coupled geochemistry of fluids and solids on Titan's surface, or if the user desires a simple model that allows new components, such as multiple solids, to be added easily.

4.2. Solubility of solid C_2H_2 in mixed solvents

Comparing models with experiments on the solubility of C_2H_2 in two-component solvents of relevance to Titan is presently inhibited by a lack of experimental data. As an alternative, we investigate the consistency of the models, as this provides information about uncertainties. The N_2–CH_4–C_2H_2 and CH_4–C_2H_6–C_2H_2 ternaries were adopted as bases for model comparisons. Only the MVL model and the model of Preston and Prausnitz (1970) are parameterized such that the solubility of solid C_2H_2 can be predicted in N_2–CH_4 and CH_4–C_2H_6 cosolvents at Titan surface temperatures. The latter model has been used extensively to estimate the concentration of C_2H_2 in lakes and hypothetical oceans on Titan (Raulin, 1987; Dubouloz et al., 1989; Cordier et al., 2009).

Calculated solubilities of solid C_2H_2 in liquid mixtures of N_2 and CH_4 at 90.6941 K are shown in Fig. 9A. There is reasonably close agreement between the MVL and Preston and Prausnitz (1970) models. Both models predict that C_2H_2 is slightly more soluble in CH_4 than in N_2. The models agree to within ~30% for N_2-rich compositions, but they deviate by as much as a factor of ~2 for CH_4-rich compositions. The former value may lie within the experimental uncertainties, but the latter value suggests that one of the models provides an inaccurate representation of the C_2H_2–CH_4 binary (the same solubility data from Neumann and Mann, 1969 were regressed). Preston and Prausnitz (1970) assumed that the empirical parameter in their model is independent of temperature, whereas the interaction energy in the MVL model varies linearly with temperature (Table 3). This difference may be responsible for the discrepancy, although a factor of ~2 may not be geochemically significant in terms of mineral solubility.

It is also informative to compare results from the MVL model with Henry's law for the ternary system, which can be written as (Prausnitz et al., 1999)

$$\log(x_3^{\text{sat}})_{\text{in mixture}} = \left(\frac{x_1}{x_1 + x_2}\right) \times \log(x_3^{\text{sat}})_{\text{in pure 1}} + \left(\frac{x_2}{x_1 + x_2}\right) \times \log(x_3^{\text{sat}})_{\text{in pure 2}}, \quad (14)$$

for the saturation mole fraction of solute 3 in a mixture of cosolvents 1 and 2. Examination of this equation reveals why the "Henry plot" in Fig. 9A is linear. In contrast, the MVL model generates a curve in Fig. 9A. Curvature is a general phenomenon in experimental ternary systems (e.g., Tiffin et al., 1979). In the present ternary, curving results in a solubility enhancement of up to ~35% relative to Henry's law. Numerical analysis of derivatives revealed that there are two reasons for curvature. The dominant factor in this case is non-ideal mixing between the cosolvents (the interaction energy for N_2–CH_4 is not zero). Therefore, the solute plays no role in creating most of the curvature. The second, minor factor here is differences in the effective volumes (i.e., sizes and shapes) of the components. This is relatively minor for N_2–CH_4–C_2H_2 because the components have similar critical volumes (Table 2).

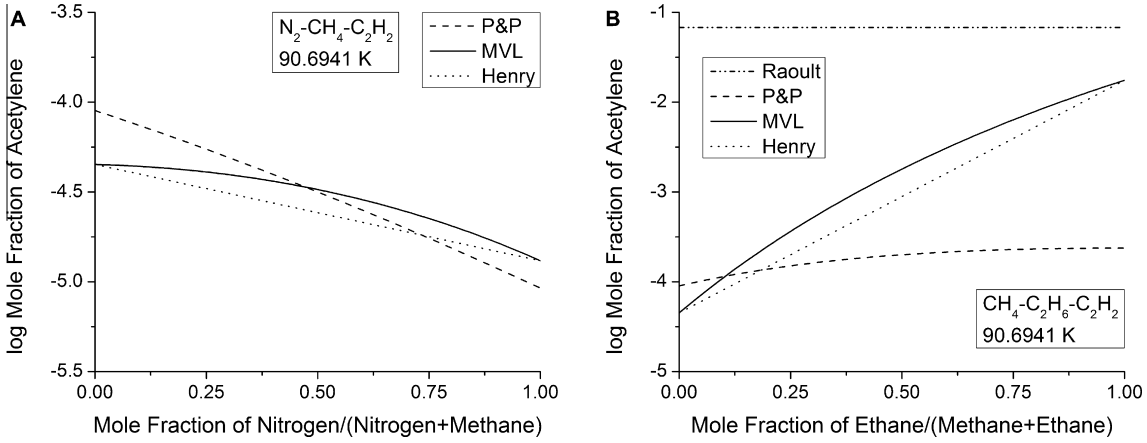

Fig. 9. Comparisons between models of the (A) N_2–CH_4–C_2H_2 and (B) CH_4–C_2H_6–C_2H_2 ternaries at 90.6941 K. Curves show predicted solubilities of solid C_2H_2 in liquids with varying proportions of the cosolvents. Henry refers to Henry's law (Eq. (14)), and Raoult refers to Raoult's law ($\gamma^{liq}_{C_2H_2} = 1$). Abbreviations: P&P, Preston and Prausnitz (1970); MVL, modified van Laar (Eq. (3)). Note the differing scales and abscissa of the plots.

Results from models of the CH_4–C_2H_6–C_2H_2 ternary at 90.6941 K are shown in Fig. 9B. There are large differences between the MVL and Preston and Prausnitz (1970) models at the C_2H_6 end of the composition scale. The MVL model predicts that C_2H_2 has a mole-fraction solubility of 1.8×10^{-2} in C_2H_6 (approaching the ideal Raoultian solubility of 6.8×10^{-2}; Eq. (10)), while the Preston and Prausnitz (1970) model predicts a solubility of 2.4×10^{-4}. At least one of the models must be incorrect! Insight can be gained by comparing these solubilities with those in pure CH_4. Preston and Prausnitz's model predicts that the solubility increases by a factor of ~3 going from CH_4 to C_2H_6, while the MVL model predicts an enhancement factor of ~390. The analogous enhancement factor for CH_4–C_2H_4 (ethylene) extrapolates to ~300 at 90.6941 K (Neumann and Mann, 1969), and the estimated enthalpy of vaporization of C_2H_2 is more similar to that of C_2H_6 (Table 2) than to that of C_2H_4 (16,389 J mol^{-1}; Smukala et al., 2000). Thus, an enhancement factor >300 seems likely for $CH_4 \rightarrow C_2H_6$. Most likely, the problem with the Preston and Prausnitz (1970) model is that the empirical parameter for C_2H_2–C_2H_6 cannot be assumed to be constant over a wide temperature range (regressed data were for 150–170 K; Clark and Din, 1950). This practice was followed in previous Titan studies and should be stopped. The solubility from the MVL model displays pronounced curvature (Fig. 9B), but differences in critical volumes (Table 2) are largely responsible for the curvature here. Overall, inconsistencies between the models stress the need for experimental solubilities of solid C_2H_2 in liquid C_2H_6 and in CH_4–C_2H_6 mixtures at Titan surface temperatures.

5. EXAMPLES OF FLUVIAL GEOCHEMISTRY ON TITAN

The thermodynamic model outlined above can be used to explore possibilities for Titan's cryogenic geochemistry. The focus in this section is the examples of solvent composition and mineral solubility that illustrate how equilibrium calculations can provide insights into the geological behavior and occurrence of materials on Titan. As on Earth, the geochemistry of materials can be expected to be linked to geological processes (Kargel, 2007; Kargel et al., 2007). Analogies to processes on Earth are made in the following discussion to aid understanding. Examples are chosen to elucidate principles using plausible values for unknown parameters. Future work will need to devote greater attention to the parameter space of temperature, pressure, and composition on Titan.

The system of interest is a CH_4–C_2H_6–C_3H_8 liquid that is in equilibrium with atmospheric N_2 and CH_4, and solid C_2H_2 (e.g., Lunine et al., 1983). We adopt the triple-point temperature of CH_4 (90.6941 K) and the atmospheric pressure (1.467 bar; Fulchignoni et al., 2005) as reference conditions. The temperature is slightly lower than that (93.65 ± 0.25 K; Fulchignoni et al., 2005) measured at the equatorial (11°S) landing site of the Huygens probe, but is similar to surface brightness temperatures in the polar regions (~90–92 K; Jennings et al., 2009). This system can be regarded as an idealized model of a polar lake or sea (Stofan et al., 2007; Turtle et al., 2009) that is in contact with C_2H_2-bearing sediments. A thermodynamic description of this system requires five constraints for the five components (or equivalently, the phase rule implies that there are four degrees of freedom). Eq. (2) is used for N_2 and CH_4, with standard state fugacities and fugacity coefficients that were parameterized to REFPROP data (Lemmon et al., 2010) [$\log(f^{\circ,liq}_{N_2}, \text{ bar}) = 3.493–268.655/T(\text{K})$, $\log(f^{\circ,liq}_{CH_4}, \text{ bar}) = 4.045–451.463/T(\text{K})$; $\phi_{N_2} = 1.063–9.17/T(\text{K})$, $\phi_{CH_4} = 1.2–26.09/T(\text{K})$]. These parameterizations are accurate to within ~1% for 85–105 K, 1.467 bar, and a mole fraction

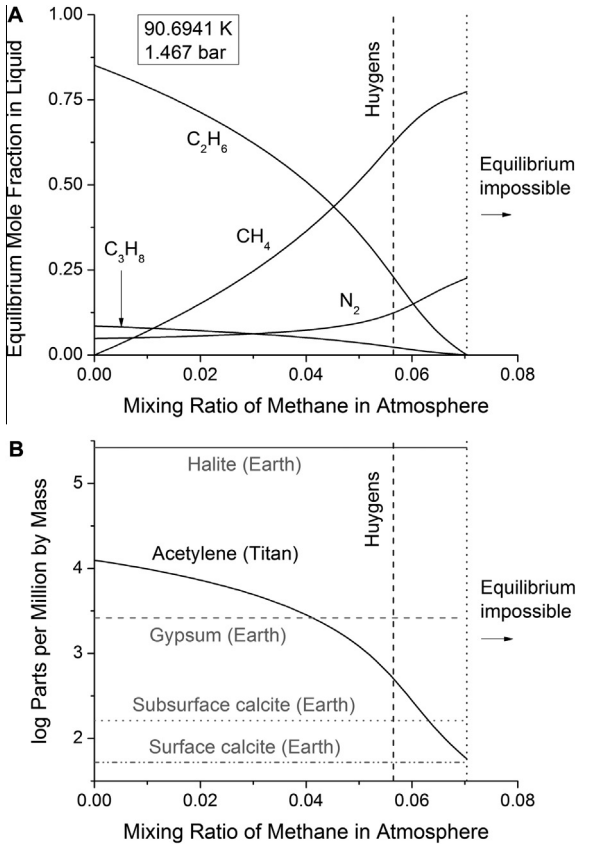

Fig. 10. (A) Predicted equilibrium composition of major components in liquids on Titan's surface, and (B) predicted solubility of solid C_2H_2 in liquids on Titan's surface, as functions of the mixing ratio (or mole fraction) of CH_4 in the near-surface atmosphere at 90.6941 K and 1.467 bar. Calculations are based on the assumptions that CH_4 and N_2 are at vapor–liquid equilibrium, liquids are saturated with respect to solid C_2H_2, and the liquid-phase mole ratio of C_2H_6/C_3H_8 is 10. The dashed vertical line labeled Huygens indicates the near-surface mixing ratio of CH_4 gas measured by the Gas Chromatograph–Mass Spectrometer onboard the Huygens probe (Niemann et al., 2010), and the dotted vertical line indicates the maximum equilibrium mixing ratio (i.e., the dew point of the N_2–CH_4 binary at these conditions). The horizontal gray lines in (B) designate solubilities of salts in pure water at Earth reference conditions (298.15 K, 1 bar). Surface calcite refers to the solubility of calcite in water at a fixed partial pressure of CO_2 of 3.9×10^{-4} bar, and subsurface calcite corresponds to a fixed partial pressure of CO_2 of 10^{-2} bar. The ppm scale was selected to facilitate comparisons between Titan and Earth.

of CH_4 gas between 0–10%. Some standard state fugacities are given in Table 2. Titan air in equilibrium with surface liquids is assumed to be a mixture of N_2 and CH_4 only (Niemann et al., 2010), and equilibrium between solid and dissolved C_2H_2 is represented by Eq. (8). The photochemical model of Lavvas et al. (2008a,b) predicts a C_2H_6/C_3H_8 mole ratio of 10 in the liquid phase, as adopted here. The final constraint is mass balance, where $\sum x_i = 1$. The four degrees of freedom are temperature, pressure, the liquid-phase mole ratio of C_2H_6/C_3H_8, and the mixing ratio of atmospheric CH_4. Five equations incorporating the preceding constraints are solved iteratively, by initially setting all of the activity coefficients to unity so that the liquid-phase mole fractions can be computed readily, then Eq. (12) is used to calculate updated activity coefficients, which are used to solve for new mole fractions. For the system of interest, activity coefficient expressions from the MVL model contain 11 terms (10 binary terms and a term for CH_4–C_2H_6–N_2; 9 ternary terms are omitted because the interaction energies are unavailable). In general, the number of binary ($j = 2$) or ternary ($j = 3$) terms for an n-component system will be

$$C = \frac{n!}{j!(n-j)!}. \tag{15}$$

5.1. Solvent species in lakes and seas at the poles

Mole fractions of CH_4, C_2H_6, C_3H_8, and N_2 in the model liquid are shown in Fig. 10A. It can be seen that either CH_4 or C_2H_6 is the dominant constituent. The crossover point occurs at a mixing ratio of atmospheric CH_4 of 4.5% (this will depend on the temperature). At higher mixing ratios, the liquid is dominated by CH_4, while C_2H_6 dominates at lower ratios. The concentration of N_2 in the liquid is sensitive to the CH_4/C_2H_6 mole ratio of the liquid. Atmospheric N_2 is predicted to be more soluble in liquids that are richer in CH_4, and the equilibrium mole fraction of N_2 in the liquid varies between 0.048 and 0.226 (Fig. 10A; based on discussions in Sections 3 and 4, calculated mole fractions of N_2 and CH_4 have maximum potential errors of ~20% and ~5%, respectively). The greater solubility in CH_4 occurs because N_2 behaves more ideally in solutions with CH_4 than in those with C_2H_6. For comparison, the solubility of atmospheric N_2 in water on Earth is $\sim 5 \times 10^{-4}$ molal or $\sim 9 \times 10^{-6}$ mole fraction at 298.15 K (Shock et al., 1989). Thus, N_2 has a much greater thermodynamic propensity to dissolve in liquids on Titan's surface than in surface waters on Earth. Reasons for this include the lower temperature, higher partial pressure of N_2, and the nonpolar solvent on Titan. The high solubility of N_2 gas in CH_4-rich liquids may have geological consequences, by altering physical (e.g., density, viscosity, heat capacity) and chemical (e.g., energy of solvation) properties of liquids on Titan. CH_4-rich liquids could also sequester significant amounts of N_2 from the atmosphere (especially if extensive "aquifers" exist; Hayes et al., 2008), which has implications for the evolution of Titan's atmosphere (e.g., Glein et al., 2009). C_3H_8 is predicted to be a less abundant constituent of surface liquids on Titan, with a maximum mole fraction of 8.5% (Fig. 10A). This value may seem small, but this concentration is considerably higher than the concentration of NaCl in seawater (~0.8 mol%; Eby, 2004). Even a brine that is saturated with respect to the mineral halite at 298.15 K contains only ~9.9 mol% of NaCl (Marion and Kargel, 2008). These comparisons draw attention to a fundamental difference between Titan and Earth. The solvent, or the major chemical composition of the naturally occurring liquid, on Titan is expected to be more complex than that on Earth, which is dominated by H_2O. It can be expected that there are mixed solvents on and near Titan's surface containing CH_4, C_2H_6, C_3H_8, and N_2, whose proportions are controlled by local physiochemical conditions (e.g., the relative humidity of CH_4).

Possible compositions of surface liquids in Titan's polar regions can be explored by comparing the results described above with determinations of mixing ratios of CH_4 gas at the surface. The Huygens GC–MS measured a mixing ratio of $(5.65 \pm 0.18) \times 10^{-2}$ for CH_4 at the probe's equatorial landing site (Niemann et al., 2010). Penteado and Griffith (2010) used a radiative transfer model to derive near-surface mixing ratios from ground-based infrared spectra, and found that CH_4 gas abundances at low and mid-latitudes are consistent with the Huygens value to within ~10–20%. If CH_4 gas is well-mixed at all latitudes, polar lakes and seas would have equilibrium compositions on the mole scale of 62.4% CH_4, 22.9% C_2H_6, 12.4% N_2, and 2.3% C_3H_8 (Fig. 10A). In this case, the liquids would be dominated by CH_4. However, mixing ratios of CH_4 gas near Titan's poles may be different from those at lower latitudes, like on Earth where water vapor in the lower troposphere is not uniformly mixed. This seems likely because the ubiquity of lakes in Titan's polar regions, and their apparent absence elsewhere (Aharonson et al., 2009; although, see Griffith et al., 2012), indicate that the polar climate is wettest, as predicted by the recent general circulation model of Schneider et al. (2012). Differences in climate imply different mixing ratios of CH_4 gas. If the CH_4 content of Titan's atmosphere is buffered by high-latitude lakes (Mitri et al., 2007), then the average mixing ratio of CH_4 in the polar atmosphere should be greater than the Huygens value, as polar air would be closer to the CH_4 source than would equatorial air. Net evaporation of CH_4 must also occur for lakes to buffer atmospheric CH_4 against photochemical destruction, which means that the lakes must be in a state of disequilibrium with respect to polar air (i.e., the actual mixing ratio of CH_4 gas is less than the equilibrium mixing ratio). Overall, the buffer model suggests that Titan's lakes and seas may be CH_4-rich (~63–77 mol%; Fig. 10A).

While spectral features consistent with the presence of liquid C_2H_6 were detected in the south polar lake Ontario Lacus, the relative abundance of C_2H_6 in the lake is not known (Brown et al., 2008), so this observation cannot be used as a quantitative constraint. The apparent shrinkage of Ontario Lacus would imply that the lake contains appreciable CH_4 if evaporation is responsible for the shrinkage, because C_2H_6 is probably not volatile enough to yield sufficient rates of evaporation (Hayes et al., 2011; although, see Cornet et al., 2012). Yet, infiltration of liquid into the subsurface could also be responsible for the loss of liquid

from Ontario Lacus, and there is insufficient information at present on the relative rates of these processes.

On the other hand, modeling of infrared data from the Voyager 1 spacecraft suggests that mixing ratios of CH_4 gas become lower at higher latitudes (~6% to ~2% from 0° to ±60°; Samuelson et al., 1997). If this model is correct, polar lakes may be rich in C_2H_6 (containing perhaps ~70 mol%; Fig. 10A), unless liquids are significantly out of equilibrium with the near-surface atmosphere. A highly dynamic polar environment (e.g., Tokano, 2009) could maintain a small actual mixing ratio of CH_4 gas despite a large equilibrium mixing ratio. Prevention of equilibrium between air and liquids would require advection of evaporated CH_4 away from polar regions and compensating input of rain to maintain a non-equilibrium steady state (evaporation and rainfall need not occur in the same place on a local scale; e.g., lakes versus highlands). A greater understanding of the relationships between the composition of surface liquids and climate can be achieved by obtaining more information about latitudinal variations in the CH_4 gas mixing ratio in the lower troposphere (especially near the poles). It should be emphasized that thermodynamic models are not restricted to systems at equilibrium. As demonstrated by this discussion, comparisons between the real system and its equilibrium state can lead to insights into processes that create disequilibrium.

Equilibrium compositions of surface liquids from several models in the Titan literature are compared in Table 4 (Lunine, 1985; Thompson, 1985; Dubouloz et al., 1989; Cordier et al., 2009; Tan et al., 2013). The comparisons are not strictly parallel because there are slight differences in temperature between the models (higher temperatures cause liquids to lose CH_4 and N_2, and gain C_2H_6). The models also have different numbers of components, so some caution is in order. In general, there is fair agreement among the models in terms of the concentrations of CH_4, C_2H_6, and N_2. Lower-temperature models generally predict that surface liquids contain more CH_4 and N_2, and less C_2H_6, as expected. Close agreement between the MVL and GERG models suggests that predictions from these models may be accurate. The anomalous model is that of Cordier et al. (2009), which predicts far less CH_4 and N_2 in the liquid phase than do the others (Table 4). Because the Cordier et al. model gives results that are significantly different from the rest of the models, it is tempting to assume that there is something incorrect with this model or its implementation. If so, the discrepancy could be attributed to: (1) potential use of inaccurate thermodynamic data; (2) incorrect numerical solutions to the equations of phase equilibrium; (3) inconsistency between model parameters and thermodynamic data; or (4) minor components in the Cordier et al. (2009) model have unrealistically large effects on the activity coefficients of major components. Note that Cordier et al. (2012) and Tan et al. (2013) also questioned the accuracy of the Cordier et al. (2009) model. Consequently, the consistency of this model with the experimental data in Supplementary Table 1 (as one example) should be determined before proceeding to Titan applications.

5.2. C_2H_2 as a mineral in sedimentary processes

The predicted solubility of solid C_2H_2 (acetylite?) in surface liquids on Titan is shown in Fig. 10B; the solubility is predicted to be a strong function of the mixing ratio of atmospheric CH_4. Solid C_2H_2 is much more soluble in liquid C_2H_6 than in liquid CH_4 (Fig. 9B), so the computed solubility of C_2H_2 is responding to changes in the composition of the solvent (Fig. 10A). This is another example of how Titan's complex solvent can influence geochemistry. One potential consequence is that, by analogy to the formation of ore deposits on Earth (Robb, 2005), mixing of liquids with different compositions could lead to the formation of deposits that are rich in C_2H_2, as well as other organic minerals on Titan. Imagine a C_2H_6-rich subsurface fluid (whose original CH_4 and N_2 were mostly driven off by mild heating) migrating through C_2H_2-bearing sediments. This fluid might contain ~10^4 ppm C_2H_2 (Fig. 10B). Mixing of this fluid with fresh meteoric fluid (e.g., 77% CH_4, 23% N_2; Fig. 10A) may cause C_2H_2 to precipitate in the mixing zone. The amount of solid formed would depend

Table 4
Comparisons between various equilibrium composition models of multicomponent liquids on Titan's surface for a CH_4 gas mixing ratio (or mole fraction) of 6% at the base of the atmosphere (i.e., similar to the Huygens value; Niemann et al., 2010). GERG refers to the GERG model (Kunz et al., 2007; Kunz and Wagner, 2012), and MVL refers to the modified van Laar model (Eq. (12)).

Variable	Lunine (1985)	Thompson (1985)	Dubouloz et al. (1989)	Cordier et al. (2009)	Tan et al. (2013)	GERG	MVL
Surface temperature (K)	94	94	92.5	93.65	93.7	90.6941	90.6941
Surface pressure (bar)	1.5	1.5	1.52	1.46	1.467	1.467	1.467
Mole percent CH_4	~50[b]	50.1	~55[b]	~7.3[b]	31.76	68.1	68.1
Mole percent C_2H_6	~41.2[b]	41.3	~35[b]	~78.3[b]	53.16	15	15.5
Mole percent C_3H_8	–	–	–	~7.6[b]	7.2	1.5	1.55
Mole percent N_2	~8.8[b]	8.6	~10[b]	~0.32[b]	6.89	15.4	14.8
Mole percent C_2H_2	⩽0.031	–	~0.02[b]	~1.18[b]	0.77	–	0.022
Mole percent others[a]	–	–	<0.01	~5.3[b]	0.22	–	–

[a] "Others" correspond to various hydrocarbons, nitriles, and inorganic compounds.
[b] Values are approximate because they were obtained by interpolating results from published figures.

on the proportions and compositions of the two fluids. Many terrestrial minerals, such as carbonates and silicates, have solubilities that are also sensitive to liquid composition. However, the activity of H^+ (i.e., pH) is usually the most important compositional variable in low-temperature aqueous geochemistry on Earth (Drever, 1997), whereas the presence of cosolvents appears to heavily influence mineral solubilities on Titan. C_2H_6 in liquid hydrocarbons on Titan is evidently the geochemical equivalent of acid in aqueous solutions on Earth, since both substances can increase the solubilities of minerals in their respective environments.

Further insights into the geochemistry of C_2H_2 on Titan can be gained by making comparisons with the solubilities of halite, gypsum, and calcite in water on Earth (Fig. 10B). The solubility of calcite in water depends on the partial pressure of CO_2. The partial pressures considered here are 3.9×10^{-4} bar (the contemporary terrestrial atmosphere), and 10^{-2} bar (a representative value for groundwaters in limestone aquifers; Garrels and Christ, 1965; Drever, 1997). Solubilities of terrestrial minerals in pure water at 298.15 K and 1 bar were calculated using the FREZCHEM model (Marion and Kargel, 2008).

Solid C_2H_2 in CH_4–N_2 meteoric fluid on Titan is about as soluble as calcite in surface waters on Earth (Fig. 10B). The solubility of C_2H_2 in liquid hydrocarbons on Titan is predicted to rival that of calcite in subsurface waters on Earth if the meteoric fluid on Titan picks up small amounts of C_2H_6 and C_3H_8 (~10 mol%) during fluid transport. This could have significant geomorphological implications. For example, Mitchell and Malaska (2011) reported that landforms consistent with karst topography, such as steep-rimmed depressions, are present in Titan's "Arctic Lake District". On Earth, karst typically develops as groundwater dissolves calcite and other carbonates in limestone (Summerfield, 1991). By analogy, our calculations suggest that dissolution of solid C_2H_2 by CH_4-rich weathering fluids could produce sinkholes or other karstic features on Titan. This will depend on many unknowns, such as the existence of thick deposits of C_2H_2-rich rock, the mechanical strength of the rock, and whether there is sufficient flow of weathering fluid through the rock. While these are difficult issues to address at present, the computed solubilities may serve as a starting point for models of solution erosion on Titan (Lorenz and Lunine, 1996; Mitchell et al., 2008; Malaska et al., 2011).

Another application of the MVL model is assessing the geochemistry of evaporite minerals on Titan. Recently, Barnes et al. (2011) discovered a 5-μm bright unit in what appear to be dry lakebeds near Titan's north pole, and proposed that the unit is composed of organic evaporites. Observations of decreasing depths and shoreline recessions of lakes with time may be consistent with evaporation or infiltration of liquid from lakes (Hayes et al., 2011; Turtle et al., 2011b; Cornet et al., 2012). Evaporation may be an agent of geochemical change on Titan (Mitri et al., 2007), as on Earth and Mars (e.g., Tosca and McLennan, 2006). Evaporation of volatile species from lakes, seas, or pore fluids will concentrate residual liquids in nonvolatile, soluble species. If the liquids become sufficiently concentrated, minerals will precipitate. An obvious difference between Earth and Titan is that evaporitic sediments are inorganic on Earth, while they should be predominately organic on Titan. Another difference is that evaporation will markedly change the composition of the solvent on Titan. Because C_2H_6 and C_3H_8 are much less volatile than CH_4 (Table 2), the proportions of C_2H_6 and C_3H_8 will increase during net evaporation of CH_4. The difference stems from the fact that natural waters on Earth do not contain appreciable amounts of nonvolatile liquids that are miscible with water. A dramatic change in solvent composition would affect evaporite geochemistry on Titan because organic mineral solubilities are expected to differ greatly between CH_4-rich and C_2H_6-rich liquids (Fig. 9B; Tiffin et al., 1979). This type of behavior is unfamiliar in terrestrial saline lakes; for instance, gypsum is only ~3.4 times more soluble in a 5 molal NaCl solution than in pure water at ambient conditions (Marion and Kargel, 2008). It is possible that some minerals on Titan could precipitate during an early stage of evaporation, but they may stop forming during later stages of evaporation after the C_2H_6 concentration has built up sufficiently in the remaining liquid. Details of how this might work would depend on the solute of interest, its initial concentration, and the starting composition of the solvent. This strange precipitation behavior may be useful for future exploration, as the process may create gaps in the sedimentary record on Titan, which may help future researchers in interpreting stratigraphic sequences.

Returning to the specific case of C_2H_2, Fig. 10B shows that solid C_2H_2 should have a solubility in C_2H_6-dominated "saline" fluids (~10^3–10^4 ppm) that is roughly comparable to that of gypsum in surface waters on Earth. Thus, C_2H_2 looks like it can be an evaporite mineral on Titan, so C_2H_2 is a logical substance to look for in putative evaporite deposits (e.g., Moriconi et al., 2010). The evaporitic character of C_2H_2 may explain why C_2H_2 has not been detected by remote sensing on the surface (Clark et al., 2010). Fluvial modification of Titan's surface may result in dissolution of solid C_2H_2, and weathering fluids may ferry C_2H_2 into the subsurface. One possible outcome is that subsurface evaporation of CH_4 may lead to precipitation of solid C_2H_2 in pore spaces of sediments, forming duricrusts by cementing sediment particles. Calcrete (calcite) and gypcrete (gypsum) duricrusts are common in deserts on Earth (Goudie, 1983; Watson, 1983), and the similar predicted solubilities of C_2H_2 (Fig. 10B) suggest that C_2H_2 could be a duricrust-former in arid regions on Titan (e.g., Lorenz et al., 2006). Note, however, that there are alternative explanations for the apparent lack of widespread C_2H_2 on Titan's surface, such as polymerization and cyclization reactions that consume C_2H_2 (Matteson, 1984; Zhou et al., 2010). This complex issue cannot be settled here, but the geochemical model has demonstrated its usefulness by suggesting a testable hypothesis that may be useful to future exploration. If C_2H_2-cemented duricrusts (acetcretes?) are present on Titan, a future robotic digger may encounter a hardened soil layer that is rich in sedimentary C_2H_2.

In closing this discussion, there are a few lingering issues to address. Will liquid solutions be at equilibrium with solids on Titan's surface? It is plausible that they may be at least close to equilibrium (e.g., Malaska and Hodyss,

2013) because relatively small energy changes are involved when nonpolar solids dissolve or precipitate. This should make it easier for molecules with even small amounts of kinetic energy to surmount activation barriers. Contrast this with minerals on Earth, where most crystal lattices are held together by strong ionic bonds, which result in large kinetic barriers for dissolution and growth processes in many cases (quartz is a notorious example). Next, calculated solubilities of solid C_2H_2 in C_2H_6-rich liquids should be regarded as provisional because the interaction energy for C_2H_2–C_2H_6 was estimated using a correlation whose accuracy remains to be fully determined (see Section 3.3). However, the predicted trend of increasing solubility with decreasing mixing ratio of CH_4 gas (Fig. 10B) is sound, as a greater proportion of C_2H_6 in the liquid (Fig. 10A) is expected to increase the solubility of solid C_2H_2 (see Section 4.2). It was emphasized in Section 5.1 that Titan's solvent is more complex than Earth's, which gives rise to unique geochemical features. It should also be pointed out that Earth's solute geochemistry is expected to be immensely richer than Titan's. On Titan, a molecule can occur in different phases, but it is still the same molecule. In contrast, ions in waters on Earth can combine in myriad ways to produce diverse secondary minerals (e.g., salts, oxyhydroxides, clay minerals). This rich combinatorial chemistry is possible because the building blocks of ionic minerals are more elementary than the formula units of minerals. For molecular minerals, such as those presumably on Titan, the two are the same. This means that the classic geochemical concepts of incongruent dissolution and chemical divides (Drever, 1997) will not apply to the geochemistry of liquid hydrocarbons on Titan.

6. CONCLUDING REMARKS

We present a generalized thermodynamic framework for quantifying phase equilibria between solids, liquids, and gases in the CH_4–C_2H_6–C_3H_8–N_2–C_2H_2 system at Titan surface conditions. The modified van Laar (MVL) model was developed to account for non-ideal behavior in liquid mixtures by calculating the activity coefficients of mixture components. Interaction energy parameters were derived by critically evaluating experimental phase equilibrium data, and regressing internally consistent data. The model provides an excellent fit to most of the data, and fits the rest of the data sufficiently well for applications to Titan. It was found that interaction energies at the triple-point temperature of CH_4 correlate linearly with differences in enthalpies of vaporization between the binary components, and this systematic behavior was exploited to estimate the interaction energies for the experimentally uncharacterized binaries C_2H_2–C_2H_6 and C_2H_2–C_3H_8. Close agreement between model predictions and experimental results for the CH_4–C_2H_6–N_2 ternary shows that the MVL model can provide accurate descriptions of non-idealities in multicomponent solutions. It was also shown that ternary data can be used to improve the model by inclusion of a ternary parameter, and that the model compares favorably to alternative models. The MVL model was applied to Titan, providing quantitative information on possible compositions of surface liquids in Titan's polar regions. Comparisons between the solubility of solid C_2H_2 in liquid hydrocarbons on Titan and the aqueous solubilities of common sedimentary salts on Earth yielded insights into the geochemistry of C_2H_2 in weathering and arid environments, with potential geological consequences of karst and evaporite formation, respectively. Overall, substantiation and demonstration of the MVL model show that it can be used to explore Titan's strange yet familiar geochemistry, which will allow quantitative assessments of how geochemical processes can produce or modify geological features on this extraordinary world.

There are numerous theoretical and experimental studies, remote observations, and *in situ* measurements that can lead to a better understanding of fluvial geochemistry on Titan:

(1) Additional binary systems at phase equilibrium should be characterized by regressing existing literature data (e.g., Hiza et al., 1982), and by obtaining new experimental data. Expanding the number of components in the MVL model will allow more complete models of geochemical processes on Titan. Such developments will also allow tests of the assumptions and correlations used in this study, leading perhaps to the development of improved predictive methods. Of special interest are binaries with CH_4 or C_2H_6, and compounds that have been detected in Titan's atmosphere (e.g., HCN; Magee et al., 2009; Coustenis et al., 2010); as well as compounds that may be present on the surface (e.g., benzene; Clark et al., 2010; Niemann et al., 2010). Geochemical models could be expanded further by considering organic products from atmospheric chemistry models (e.g., Lavvas et al., 2008a,b) and experiments (e.g., Thompson et al., 1991), as well as cosmochemically abundant ices and noble gases. A speculative class of surface materials is organometallic compounds (e.g., ferrocene, iron pentacarbonyl), which could form from delivery of metals by comets or interplanetary dust. It is also recommended that compounds with diverse structural or electronic properties be studied to obtain fundamental information about non-ideal behavior in cryogenic solutions.

(2) Phase equilibrium experiments with ternary mixtures at Titan surface conditions would provide data that can be used to test the MVL model more thoroughly, refine the model, or call for new approaches. Of greatest relevance to Titan are ternaries with liquid CH_4 and C_2H_6, especially equimolar mixtures.

(3) Determining whether relevant organic solids can form appreciable solid solutions at Titan surface conditions (e.g., Hodyss et al., 2013) will affect the thermodynamic treatment adopted here (see Eq. (8)). It might be expected that substances can form a solid solution if they have identical crystal structures, and similar critical volumes and chemical characteristics.

(4) Extension of the MVL model to higher temperatures and pressures will permit computational studies of thermally-driven geochemical processes in Titan's

subsurface. This could lead to insights into possible diagenetic mechanisms for producing sedimentary rocks (e.g., sandstones), such as precipitation of cements during cooling of fluids that are saturated with respect to organic minerals. In addition, organic minerals that precipitate at higher temperatures could serve as spectral markers that may help in identifying current or past regions of elevated thermal activity using remote sensing.

(5) More comprehensive modeling of phase equilibria would lead to a more detailed understanding of how Titan's cryogenic geochemistry might respond to changes in geochemical variables. This, in turn, could drive hypotheses about the wider context of fluvial geochemistry on hydrocarbon worlds in the Universe. Such greasy worlds may be common (Lunine, 2010), especially around stars that have a higher carbon-to-oxygen ratio than the Sun (e.g., Johnson et al., 2012). Another potentially fruitful application would be to constrain the bioenergetics of speculative life in liquid hydrocarbons (McKay and Smith, 2005) using standard Gibbs energies of formation (Table 2) together with the MVL model.

(6) Laboratory studies of kinetic phenomena, such as rates of evaporation of CH_4 (Luspay-Kuti et al., 2012) and rates of dissolution of relevant organic solids in liquid CH_4 and C_2H_6 (Malaska and Hodyss, 2013), will help in clarifying the appropriateness of the equilibrium assumption under various conditions. Experiments could also examine equilibrium and kinetic isotopic fractionations. As an example, there may be a meteoric methane line on Titan that is analogous to the meteoric water line on Earth (Craig, 1961), so experiments could provide lessons on how the isotopic composition of CH_4 evolves in response to non-equilibrium processes. Precipitation of minerals may also fractionate isotopes appreciably, implying that the isotopic composition of minerals may constitute a record of geochemical conditions in Titan's past.

(7) Our ability to simulate actual geochemical processes on Titan is hampered by limited knowledge of the composition of Titan's surface. Unambiguous identification of surface materials will most likely require *in situ* measurements. Crucial pieces of information are the compositions, proportions, and distributions of liquids and solids, as functions of local climate and geology. The ethane-to-methane ratio in Titan's lakes is particularly important (Soderblom et al., 2012). As on Earth, a great deal could be learned about how liquids evolve geochemically by comparing the molecular and isotopic compositions of Titan's air, rain, rivers, lakes, seas, and subsurface fluids.

(8) Finally, further exploration of Titan's CH_4-based volatile cycle (at present and in the past) is called for to enable more detailed assessments of its potential for supporting diverse types of geochemistry. Continued geomorphological studies of fluvial landforms and associated features, observations of seasonal changes in tropospheric clouds and liquid bodies such as lakes, and models of the climate and carbon cycle will all be helpful.

ACKNOWLEDGMENTS

The research reported above represents part of the first author's Ph.D. dissertation at Arizona State University. Funding for this work was provided by the National Aeronautics and Space Administration Exobiology and Evolutionary Biology program (Grant NNX10AJ29G). We thank Sugata Tan for providing results from his thermodynamic model, Misha Zolotov and Hilairy Hartnett for constructive comments on an early draft of the manuscript, John Prausnitz for some early advice on thermodynamic modeling, and Mark Ghiorso and two anonymous referees for helpful reviews. This project was inspired by the brilliant, pioneering studies of fluid-phase equilibria on Titan by the late W. Reid Thompson.

APPENDIX A. DERIVATION OF THE MODIFIED VAN LAAR MODEL

Here, we show how Scatchard–Hildebrand regular solution theory can be transformed into the modified van Laar (MVL) model. Regular solution theory provides a suitable basis for an empirical model of non-ideal behavior in mixtures of nonpolar molecules. This theory assumes that the volume of a liquid mixture is the sum of pure-component volumes, and the entropy of mixing of pure components is equivalent to that of the corresponding ideal solution. The distribution and orientations of molecules are random in a regular solution, as a result of non-directional intermolecular interactions and thermal agitation. In general, these assumptions are appropriate for mixtures of nonpolar molecules (Hildebrand and Scott, 1950). The excess Gibbs energy of mixing (G^E) refers to the difference in Gibbs energy between a solution and its ideal counterpart. In Scatchard–Hildebrand theory, G^E for binary 1–2 is given by (Prausnitz et al., 1999)

$$\frac{G^E}{v_{\mathrm{mix}}} = \left(\frac{\Delta U_1}{v_1} + \frac{\Delta U_2}{v_2} - 2\frac{\Delta U_{12}}{v_{12}}\right)\Phi_1\Phi_2, \tag{A1}$$

where ΔU_i stands for the internal energy of vaporization of component i to the ideal gas state, v_i designates the liquid volume of component i at the temperature and pressure of the system, and Φ_i indicates the volume fraction of component i in the mixture. Parameters with subscript 12 are constants that are used with mixing rules to characterize mixtures in terms of pure-component properties. Volume v_{12} can be decomposed using the van der Waals mixing rule for volume parameters: $v_{12} = (v_1 + v_2)/2$. Substituting this into Eq. (A1) and rearranging, yields

$$\frac{G^E}{v_{\mathrm{mix}}} = \frac{\omega_{12}\Phi_1\Phi_2}{v_1 + v_2}, \tag{A2}$$

where

$$\omega_{12} = \left(1 + \frac{v_2}{v_1}\right)\Delta U_1 + \left(1 + \frac{v_1}{v_2}\right)\Delta U_2 - 4\Delta U_{12}, \tag{A3}$$

and ω_{12} is defined as the interaction energy for binary 1–2. To obtain optimal agreement with experimental data, ω_{12} is treated as an adjustable parameter (e.g., Peng, 2010). Theoretical evaluation of ω_{12} is hampered by the inability to formulate a suitable mixing rule for ΔU_{12} (arithmetic and geometric means are insufficient). A second modification of regular solution theory is to replace liquid volumes in Eq. (A2) with effective volumes (q), as suggested by Hildebrand and Scott (1950). This gives the MVL model more flexibility.

A simple and useful expression for the excess Gibbs energy of mixing in multicomponent systems from the MVL model is

$$\frac{G^E}{q_{\text{mix}}} = \sum_{i=1}^{n-1}\sum_{j>i}^{n}\frac{\omega_{ij} z_i z_j}{q_i + q_j}, \tag{A4}$$

where z_i represents the effective volume fraction of component i in the mixture. Activity coefficients (i.e., Eq. (3)) can be derived from Eq. (A4) by differentiating Eq. (A4) with respect to the component of interest (see Prausnitz et al., 1999). This guarantees thermodynamic consistency by satisfying the Gibbs–Duhem equation. Summing binary contributions to non-ideal behavior in Eq. (A4) should provide acceptable approximations for nonpolar mixtures, in which two-body interactions dominate because relatively weak dispersion forces between nonpolar molecules act over short distances.

The accuracy of the MVL model can be improved by accounting for ternary interactions. A logical extension of Eq. (A4) is (e.g., Wohl, 1946)

$$\frac{G^E}{q_{\text{mix}}} = \sum_{i=1}^{n-1}\sum_{j>i}^{n}\frac{\omega_{ij} z_i z_j}{q_i + q_j} + \sum_{a=1}^{n-2}\sum_{b>a}^{n-1}\sum_{c>b}^{n}\frac{\omega_{abc} z_a z_b z_c}{q_a + q_b + q_c}, \tag{A5}$$

where ω_{abc} specifies the interaction energy for ternary a–b–c. This is a more general form of the MVL model. The structure of this equation is reminiscent of that used in the formulation of the Pitzer equations (Pitzer, 1973), which are used in geochemistry to calculate the activity coefficients of components in saline solutions (e.g., Harvie et al., 1984). There is also an analogy with the virial equation (Prausnitz et al., 1999). Differentiation of Eq. (A5) leads to Eq. (12). Adding further corrections, such as quaternary terms, seems unnecessary for nonpolar mixtures, and would make the model unwieldy.

APPENDIX B. SUPPLEMENTARY DATA

Supplementary data associated with this article can be found, in the online version, at http://dx.doi.org/10.1016/j.gca.2013.03.030.

REFERENCES

Aharonson O., Hayes A. G., Lunine J. I., Lorenz R. D., Allison M. D. and Elachi C. (2009) An asymmetric distribution of lakes on Titan as a possible consequence of orbital forcing. *Nat. Geosci.* **2**, 851–854.

Ambrose D. (1956) The vapour pressures and critical temperatures of acetylene and carbon dioxide. *Trans. Faraday Soc.* **52**, 772–781.

Ambrose D. and Townsend R. (1964) Vapour pressure of acetylene. *Trans. Faraday Soc.* **60**, 1025–1029.

Anderson G. M. (2005) *Thermodynamics of Natural Systems*. Cambridge University Press, New York.

Barker J. A. (1953) Determination of activity coefficients from total pressure measurements. *Aust. J. Chem.* **6**, 207–210.

Barnes J. W., Bow J., Schwartz J., Brown R. H., Soderblom J. M., Hayes A. G., Vixie G., Le Mouelic S., Rodriguez S., Sotin C., Jaumann R., Stephan K., Soderblom L. A., Clark R. N., Buratti B. J., Baines K. H. and Nicholson P. D. (2011) Organic sedimentary deposits in Titan's dry lakebeds: probable evaporite. *Icarus* **216**, 136–140.

Black C. (1958) Phase equilibria in binary and multicomponent systems: modified van Laar-type equation. *Ind. Eng. Chem.* **50**, 403–412.

Bourbo P. S. (1943) Vapor pressure of solid acetylene. *J. Phys. – USSR* **7**, 286–288.

Brown R. H., Soderblom L. A., Soderblom J. M., Clark R. N., Jaumann R., Barnes J. W., Sotin C., Buratti B., Baines K. H. and Nicholson P. D. (2008) The identification of liquid ethane in Titan's Ontario Lacus. *Nature* **454**, 607–610.

Bucker D. and Wagner W. (2006) A reference equation of state for the thermodynamic properties of ethane for temperatures from the melting line to 675 K and pressures up to 900 MPa. *J. Phys. Chem. Ref. Data* **35**, 205–266.

Calado J. C. G., Garcia G. A. and Staveley L. A. K. (1974) Thermodynamics of the liquid system methane + propane. *J. Chem. Soc. Faraday Trans. I* **70**, 1445–1451.

Chang S. D. and Lu B. C. Y. (1967) Vapor–liquid equilibria in the nitrogen–methane–ethane system. *Chem. Eng. Prog. Symp. Ser.* **63**, 18–27.

Chao J., Wilhoit R. C. and Zwolinski B. J. (1973) Ideal gas thermodynamic properties of ethane and propane. *J. Phys. Chem. Ref. Data* **2**, 427–437.

Chase, Jr., M. W. (1998) NIST-JANAF thermochemical tables. *J. Phys. Chem. Ref. Data, Monograph No. 9*. American Institute of Physics, New York.

Cheung H. and Wang D. I. J. (1964) Solubility of volatile gases in hydrocarbon solvents at cryogenic temperatures. *Ind. Eng. Chem. Fundam.* **3**, 355–361.

Chien H. H. Y. and Null H. R. (1972) Generalized multicomponent equation for activity coefficient calculation. *Am. Inst. Chem. Eng. J.* **18**, 1177–1183.

Clark A. M. and Din F. (1950) Equilibria between solid, liquid, and gaseous phases at low temperatures. Binary systems acetylene–carbon dioxide, acetylene–ethylene and acetylene–ethane. *Trans. Faraday Soc.* **46**, 901–911.

Clark R. N., Curchin J. M., Barnes J. W., Jaumann R., Soderblom L., Cruikshank D. P., Brown R. H., Rodriguez S., Lunine J., Stephan K., Hoefen T. M., Le Mouelic S., Sotin C., Baines K. H., Buratti B. J. and Nicholson P. D. (2010) Detection and mapping of hydrocarbon deposits on Titan. *J. Geophys. Res.* **115**, E10005. http://dx.doi.org/10.1029/2009JE003369.

CODATA (Committee on Data for Science and Technology) (2010) *Internationally Recommended Values of Fundamental Physical Constants*. 21 Mar. 2012. <http://physics.nist.gov/cuu/Constants/index.html>.

Cordier D., Mousis O., Lunine J. I., Lavvas P. and Vuitton V. (2009) An estimate of the chemical composition of Titan's lakes. *Astrophys. J. Lett.* **707**, L128–L131.

Cordier D., Mousis O., Lunine J. I., Lebonnois S., Lavvas P., Lobo L. Q. and Ferreira A. G. M. (2010) About the possible role of hydrocarbon lakes in the origin of Titan's noble gas atmospheric depletion. *Astrophys. J. Lett.* **721**, L117–L120.

Cordier D., Mousis O., Lunine J. I., Lebonnois S., Rannou P., Lavvas P., Lobo L. Q. and Ferreira A. G. M. (2012) Titan's

lakes chemical composition: sources of uncertainties and variability. *Planet. Space Sci.* **61**, 99–107.

Cornet T., Bourgeois O., Le Mouelic S., Rodriguez S., Sotin C., Barnes J. W., Brown R. H., Baines K. H., Buratti B. J., Clark R. N. and Nicholson P. D. (2012) Edge detection applied to Cassini images reveals no measurable displacement of Ontario Lacus' margin between 2005 and 2010. *J. Geophys. Res.* **117**, E07005. http://dx.doi.org/10.1029/2012JE004073.

Coustenis A. et al. (2009) TandEM: Titan and Enceladus mission. *Exp. Astron.* **23**, 893–946.

Coustenis A., Jennings D. E., Nixon C. A., Achterberg R. K., Lavvas P., Vinatier S., Teanby N. A., Bjoraker G. L., Carlson R. C., Piani L., Bampasidis G., Flasar F. M. and Romani P. N. (2010) Titan trace gaseous composition from CIRS at the end of the Cassini–Huygens prime mission. *Icarus* **207**, 461–476.

Craig H. (1961) Isotopic variations in meteoric waters. *Science* **133**, 1702–1703.

Cutler A. J. B. and Morrison J. A. (1965) Excess thermodynamic functions for liquid mixtures of methane + propane. *Trans. Faraday Soc.* **61**, 429–442.

Diez y Riega M. H. (2010) Solubility and spectroscopy of unsaturated hydrocarbons in cryogenic solvents. Ph. D. thesis, Baylor Univ.

Djordjevich L. and Budenholzer R. A. (1970) Vapor–liquid equilibrium data for ethane–propane system at low temperatures. *J. Chem. Eng. Data* **15**, 10–12.

Drever J. I. (1997) *The Geochemistry of Natural Waters: Surface and Groundwater Environments*. Prentice Hall, Upper Saddle River, New Jersey.

Dubouloz N., Raulin F., Lellouch E. and Gautier D. (1989) Titan's hypothesized ocean properties: the influence of surface temperature and atmospheric composition uncertainties. *Icarus* **82**, 81–96.

Eby G. N. (2004) *Principles of Environmental Geochemistry*. Brooks/Cole, Belmont, California.

Elachi C., Wall S., Janssen M., Stofan E., Lopes R., Kirk R., Lorenz R., Lunine J., Paganelli F., Soderblom L., Wood C., Wye L., Zebker H., Anderson Y., Ostro S., Allison M., Boehmer R., Callahan P., Encrenaz P., Flamini E., Francescetti G., Gim Y., Hamilton G., Hensley S., Johnson W., Kelleher K., Muhleman D., Picardi G., Posa F., Roth L., Seu R., Shaffer S., Stiles B., Vetrella S. and West R. (2006) Titan Radar Mapper observations from Cassini's T_3 fly-by. *Nature* **441**, 709–713.

Ellington R. T., Eakin B. E., Parent J. D. and Gami D. C. (1959) Vapor–liquid phase equilibria in the binary systems of methane, ethane and nitrogen. In *Thermodynamic and Transport Properties of Gases, Liquids and Solids*. The American Society of Mechanical Engineers, New York, pp. 180–194.

Fedorova M. F. (1940) Solubility of acetylene and carbon dioxide in liquid nitrogen and liquid oxygen. *Zh. Fiz. Khim.* **14**, 422–426.

Focke W. W. (2001) Local composition structured fluid model for the excess Gibbs energy of liquid mixtures. *Ind. Eng. Chem. Res.* **40**, 2971–2981.

Fuks S. and Bellemans A. (1967) Excess free energies and volumes of two simple binary liquid mixtures: methane–krypton and nitrogen–methane. *Bull. Soc. Chim. Belg.* **76**, 290–299.

Fulchignoni M., Ferri F., Angrilli F., Ball A. J., Bar-Nun A., Barucci M. A., Bettanini C., Bianchini G., Borucki W., Colombatti G., Coradini M., Coustenis A., Debei S., Falkner P., Fanti G., Flamini E., Gaborit V., Grard R., Hamelin M., Harri A. M., Hathi B., Jernej I., Leese M. R., Lehto A., Lion Stoppato P. F., Lopez-Moreno J. J., Makinen T., McDonnell J. A. M., McKay C. P., Molina-Cuberos G., Neubauer F. M., Pirronello V., Rodrigo R., Saggin B., Schwingenschuh K., Seiff A., Simoes F., Svedhem H., Tokano T., Towner M. C., Trautner, Withers P. and Zarnecki J. C. (2005) In situ measurements of the physical characteristics of Titan's environment. *Nature* **438**, 785–791.

Gabis D. H. (1991) Liquid–vapor equilibrium at 90–160 K for systems containing nitrogen, methane, and ethane. M. S. thesis, Cornell Univ.

Garrels R. M. and Christ C. L. (1965) *Solutions, Minerals, and Equilibria*. Freeman, Cooper & Company, San Francisco, California.

Gasem K. A. M., Hiza M. J. and Kidnay A. J. (1981) Phase behavior in the nitrogen + ethylene system from 120 to 200 K. *Fluid Phase Equilib.* **6**, 181–189.

Glein C. R., Desch S. J. and Shock E. L. (2009) The absence of endogenic methane on Titan and its implications for the origin of atmospheric nitrogen. *Icarus* **204**, 637–644.

Gomes de Azevedo E. J. S. and Calado J. C. G. (1989) Thermodynamics of liquid methane + ethane. *Fluid Phase Equilib.* **49**, 21–34.

Goudie A. S. (1983) Calcrete. In *Chemical Sediments and Geomorphology: Precipitates and Residua in the Near-Surface Environment* (eds. A. S. Goudie and K. Pye). Academic Press, New York, pp. 93–131.

Griffith C. A., Lora J. M., Turner J., Penteado P. F., Brown R. H., Tomasko M. G., Doose L. and See C. (2012) Possible tropical lakes on Titan from observations of dark terrain. *Nature* **486**, 237–239.

Guedes H. J. R., Zollweg J. A., Filipe E. J. M., Martins L. F. G. and Calado J. C. G. (2002) Thermodynamics of liquid (nitrogen + ethane). *J. Chem. Thermodyn.* **34**, 669–678.

Harvie C. E., Moller N. and Weare J. H. (1984) The prediction of mineral solubilities in natural waters: the Na–K–Mg–Ca–H–Cl–SO_4–OH–HCO_3–CO_3–CO_2–H_2O system to high ionic strengths at 25 °C. *Geochim. Cosmochim. Acta* **48**, 723–751.

Hayes A., Aharonson O., Callahan P., Elachi C., Gim Y., Kirk R., Lewis K., Lopes R., Lorenz R., Lunine J., Mitchell K., Mitri G., Stofan E. and Wall S. (2008) Hydrocarbon lakes on Titan: distribution and interaction with a porous regolith. *Geophys. Res. Lett.* **35**, L09204. http://dx.doi.org/10.1029/2008GL033409.

Hayes A. G., Aharonson O., Lunine J. I., Kirk R. L., Zebker H. A., Wye L. C., Lorenz R. D., Turtle E. P., Paillou P., Mitri G., Wall S. D., Stofan E. R., Mitchell K. L. and Elachi C. and the Cassini RADAR Team (2011) Transient surface liquid in Titan's polar regions from Cassini. *Icarus* **211**, 655–671.

Heintz A. and Bich E. (2009) Thermodynamics in an icy world: the atmosphere and internal structure of Saturn's moon Titan. *Pure Appl. Chem.* **81**, 1903–1920.

Hildebrand J. H. (1927) A quantitative treatment of deviations from Raoult's law. *Proc. Natl. Acad. Sci.* **13**, 267–272.

Hildebrand J. H. and Scott R. L. (1950) *The Solubility of Nonelectrolytes*. Reinhold Publishing Corporation, New York.

Hiza M. J., Miller R. C. and Kidnay A. J. (1979) A review, evaluation, and correlation of the phase equilibria, heat of mixing, and change in volume on mixing for liquid mixtures of methane + ethane. *J. Phys. Chem. Ref. Data* **8**, 799–816.

Hiza M. J., Kidnay A. J. and Miller R. C. (1982) *Equilibrium Properties of Fluid Mixtures 2: A Bibliography of Experimental Data on Selected Fluids*. IFI/Plenum, New York.

Hodyss R., Johnson P. V. and Kanik I. (2010) Experimental determination of the solubilities of organics and rare gases in simulated Titan lake solutions. *Astrobiol. Sci. Conf.* #5294 (abstr.).

Hodyss R., Choukroun M., Sotin C. and Beauchamp P. (2012) The solubility of ^{40}Ar in liquid hydrocarbons: implications for Titan's geological evolution. In *Titan Through Time 2 Workshop* (eds. V. Cottini, C. Nixon and R. Lorenz). #80 (abstr.).

Hodyss R., Choukroun M., Beauchamp P. and Sotin C. (2013) Titan's beaches: an examination of what is possible and what is chemically feasible. *Lunar Planet. Sci. Conf.* #1164 (abstr.).

Holland T. and Powell R. (2003) Activity-composition relations for phases in petrological calculations: an asymmetric multicomponent formulation. *Contrib. Mineral. Petrol.* **145**, 492–501.

Houssin-Agbomson D., Coquelet C., Richon D. and Arpentinier P. (2010) Equipment using a "static–analytic" method for solubility measurements in potentially hazardous binary mixtures under cryogenic temperatures. *Cryogenics* **50**, 248–256.

Ishkin I. P. and Burbo P. Z. (1939) Solubility of solid acetylene and carbon dioxide in liquid oxygen, nitrogen and oxygen–nitrogen mixtures. *Zh. Fiz. Khim.* **13**, 1337–1339.

Jaumann R., Kirk R. L., Lorenz R. D., Lopes R. M. C., Stofan E., Turtle E. P., Keller H. U., Wood C. A., Sotin C., Soderblom L. A. and Tomasko M. G. (2009) Geology and surface processes on Titan. In *Titan from Cassini–Huygens* (eds. R. H. Brown, J. P. Lebreton and J. H. Waite). Springer, New York, pp. 75–140.

Jennings D. E., Flasar F. M., Kunde V. G., Samuelson R. E., Pearl J. C., Nixon C. A., Carlson R. C., Mamoutkine A. A., Brasunas J. C., Guandique E., Achterberg R. K., Bjoraker G. L., Romani P. N., Segura M. E., Albright S. A., Elliot M. H., Tingley J. S., Calcutt S., Coustenis A. and Courtin R. (2009) Titan's surface brightness temperatures. *Astrophys. J. Lett.* **691**, L103–L105.

Johnson T. V., Mousis O., Lunine J. I. and Madhusudhan N. (2012) Planetesimal compositions in exoplanet systems. *Astrophys. J.* **757**, 192. http://dx.doi.org/10.1088/0004-637X/757/2/192.

Kargel J. S. (2007) Theory of geochemical/geological homology applied to hydrocarbon and organic substances on icy satellites and other solid planetary objects. *Worksh. Ices, Oceans, and Fire: Satellites of the Outer Solar, System*. #6084 (abstr.).

Kargel J. S., Furfaro R., Hays C. C., Lopes R. M. C., Lunine J. I., Mitchell K. L., Wall S. D. and the Cassini RADAR Team. (2007) Titan's goo-sphere: glacial, permafrost, evaporite, and other familiar processes involving exotic materials. *Lunar Planet. Sci. Conf.* #1992 (abstr.).

Kidnay A. J., Miller R. C., Sloan E. D. and Hiza M. J. (1985) A review and evaluation of the phase equilibria, liquid-phase heats of mixing and excess volumes, and gas-phase PVT measurements for nitrogen + methane. *J. Phys. Chem. Ref. Data* **14**, 681–694.

Kouvaris L. C. and Flasar F. M. (1991) Phase equilibrium of methane and nitrogen at low temperatures: application to Titan. *Icarus* **91**, 112–124.

Kremer H. and Knapp H. (1983) Three-phase conditions are predictable. *Hydrocarbon Process.* **62**, 79–83.

Kunz O. and Wagner W. (2012) The GERG-2008 wide-range equation of state for natural gases and other mixtures: an expansion of GERG-2004. *J. Chem. Eng. Data* **57**, 3032–3091.

Kunz O., Klimeck R., Wagner W. and Jaeschke M. (2007) The GERG-2004 wide-range equation of state for natural gases and other mixtures, GERG TM-15. Fortschr.-Ber. VDI, Reihe 6, Nr. 557, VDI Verlag, Dusseldorf, Germany.

Langhans M. H., Jaumann R., Stephan K., Brown R. H., Buratti B. J., Clark R. N., Baines K. H., Nicholson P. D., Lorenz R. D., Soderblom L. A., Soderblom J. M., Sotin C., Barnes J. W. and Nelson R. (2012) Titan's fluvial valleys: morphology, distribution, and spectral properties. *Planet. Space Sci.* **60**, 34–51.

Lavvas P. P., Coustenis A. and Vardavas I. M. (2008a) Coupling photochemistry with haze formation in Titan's atmosphere, Part I: model description. *Planet. Space Sci.* **56**, 27–66.

Lavvas P. P., Coustenis A. and Vardavas I. M. (2008b) Coupling photochemistry with haze formation in Titan's atmosphere, Part II: results and validation with Cassini/Huygens data. *Planet. Space Sci.* **56**, 67–99.

Lemmon E. W., McLinden M. O. and Wagner W. (2009) Thermodynamic properties of propane. III. A reference equation of state for temperatures from the melting line to 650 K and pressures up to 1000 MPa. *J. Chem. Eng. Data* **54**, 3141–3180.

Lemmon E. W., Huber M. L. and McLinden M. O. (2010) *NIST Standard Reference Database 23: Reference Fluid Thermodynamic and Transport Properties-REFPROP*, Version 9.0. National Institute of Standards and Technology, Standard Reference Data Program, Gaithersburg, Maryland.

Llave F. M., Luks K. D. and Kohn J. P. (1985) Three-phase liquid–liquid–vapor equilibria in the binary systems nitrogen + ethane and nitrogen + propane. *J. Chem. Eng. Data* **30**, 435–438.

Llave F. M., Luks K. D. and Kohn J. P. (1987) Three-phase liquid–liquid–vapor equilibria in the nitrogen + methane + ethane and nitrogen + methane + propane systems. *J. Chem. Eng. Data* **32**, 14–17.

Lorenz R. D. and Lunine J. I. (1996) Erosion on Titan: past and present. *Icarus* **122**, 79–91.

Lorenz R. D., Wall S., Radebaugh J., Boubin G., Reffet E., Janssen M., Stofan E., Lopes R., Kirk R., Elachi C., Lunine J., Mitchell K., Paganelli F., Soderblom L., Wood C., Wye L., Zebker H., Anderson Y., Ostro S., Allison M., Boehmer R., Callahan P., Encrenaz P., Ori G. G., Francescetti G., Gim Y., Hamilton G., Hensley S., Johnson W., Kelleher K., Muhleman D., Picardi G., Posa F., Roth L., Seu R., Shaffer S., Stiles B., Vetrella S., Flamini E. and West R. (2006) The sand seas of Titan: Cassini RADAR observations of longitudinal dunes. *Science* **312**, 724–727.

Lorenz R. D., Lopes R. M., Paganelli F., Lunine J. I., Kirk R. L., Mitchell K. L., Soderblom L. A., Stofan E. R., Ori G., Myers M., Miyamoto H., Radebaugh J., Stiles B., Wall S. D., Wood C. A. and the Cassini RADAR Team. (2008a) Fluvial channels on Titan: Initial Cassini RADAR observations. *Planet. Space Sci.* 56, 1132–1144.

Lorenz R. D., Mitchell K. L., Kirk R. L., Hayes A. G., Aharonson O., Zebker H. A., Paillou P., Radebaugh J., Lunine J. I., Janssen M. A., Wall S. D., Lopes R. M., Stiles B., Ostro S., Mitri G. and Stofan E. R. (2008b) Titan's inventory of organic surface materials. *Geophys. Res. Lett.* **35**, L02206. http://dx.doi.org/10.1029/2007GL032118.

Lunine J. I. (1985) Volatiles in the outer solar system: I. Thermodynamics of Clathrate Hydrates. II. Ethane ocean on Titan. III. Evolution of primordial Titan atmosphere. Ph. D. thesis, California Institute of Technology.

Lunine J. I. (2010) Titan and habitable planets around M-dwarfs. *Faraday Discuss.* **147**, 405–418.

Lunine J. I. and Lorenz R. D. (2009) Rivers, lakes, dunes, and rain: crustal processes in Titan's methane cycle. *Annu. Rev. Earth Planet. Sci.* **37**, 299–320.

Lunine J. I., Stevenson D. J. and Yung Y. L. (1983) Ethane Ocean on Titan. *Science* **222**, 1229–1230.

Luspay-Kuti A., Chevrier V. F., Wasiak F. C., Roe L. A., Welivitiya W. D. D. P., Cornet T., Singh S. and Rivera-Valentin E. G. (2012) Experimental simulations of CH_4 evaporation on Titan. *Geophys. Res. Lett.* **39**, L23203. http://dx.doi.org/10.1029/2012GL054003.

Magee B. A., Waite J. H., Mandt K. E., Westlake J., Bell J. and Gell D. A. (2009) INMS-derived composition of Titan's upper atmosphere: analysis methods and model comparison. *Planet. Space Sci.* **57**, 1895–1916.

Malaska M. and Hodyss R. (2013) Laboratory investigation of benzene dissolving in a Titan ethane lake. *Lunar Planet. Sci. Conf.* #2744 (abstr.).

Malaska M., Radebaugh J., Mitchell K., Lopes R., Wall S. and Lorenz R. (2011) Surface dissolution model for Titan karst. *First Int. Planet. Cave Res. Worksh.* #8018 (abstr.).

Marion G. M. and Kargel J. S. (2008) *Cold Aqueous Planetary Geochemistry with FREZCHEM: From Modeling to the Search for Life at the Limits*. Springer, Berlin.

Matteson D. S. (1984) Acetylene on Titan. *Science* **223**, 1131.

McClure D. W., Lewis K. L., Miller R. C. and Staveley L. A. K. (1976) Excess enthalpies and Gibbs free energies for nitrogen + methane at temperatures below the critical point of nitrogen. *J. Chem. Thermodyn.* **8**, 785–792.

McIntosh D. (1907) The physical properties of liquid and solid acetylene. *J. Phys. Chem.* **11**, 306–317.

McKay C. P. and Smith H. D. (2005) Possibilities for methanogenic life in liquid methane on the surface of Titan. *Icarus* **178**, 274–276.

McKay C. P., Pollack J. B., Lunine J. I. and Courtin R. (1993) Coupled atmosphere-ocean models of Titan's past. *Icarus* **102**, 88–98.

Miller R. C. and Staveley L. A. K. (1976) Excess enthalpies for some binary liquid mixtures of low-molecular-weight alkanes. *Adv. Cryog. Eng.* **21**, 493–500.

Miller R. C., Kidnay A. J. and Hiza M. J. (1980) A review, evaluation, and correlation of the phase equilibria, heat of mixing, and change in volume on mixing for liquid mixtures of methane + propane. *J. Phys. Chem. Ref. Data* **9**, 721–734.

Miskiewicz S., Rieser K. and Dorfmuller T. (1976) Thermodynamic studies on condensed phases. *Ber. Bunsen Ges.* **80**, 395–405.

Mitchell K. L. and Malaska M. (2011) Karst on Titan. *First Int. Planet. Cave Res. Worksh.* #8021 (abstr.).

Mitchell K. L., Lopes R. M. C., Radebaugh J., Lorenz R. D., Stofan E. R., Wall S. D., Kargel J. S., Kirk R. L., Lunine J. I., Ostro S. J., Farr T. G. and the Cassini RADAR Team (2008) The formation of high latitude karst lakes on Titan and implications for the existence of polar caps. *Lunar Planet. Sci. Conf.* #2170 (abstr.).

Mitri G., Showman A. P., Lunine J. I. and Lorenz R. D. (2007) Hydrocarbon lakes on Titan. *Icarus* **186**, 385–394.

Moriconi M. L., Lunine J. I., Adriani A., D'Aversa E., Negrao A., Filacchione G. and Coradini A. (2010) Characterization of Titan's Ontario Lacus region from Cassini/VIMS observations. *Icarus* **210**, 823–831.

Neumann A. and Mann R. (1969) Solubility of solid acetylene in liquid methane–ethylene mixtures. *Chem. Ing. Tech.* **41**, 708–711.

Niemann H. B., Atreya S. K., Demick J. E., Gautier D., Haberman J. A., Harpold D. N., Kasprzak W. T., Lunine J. I., Owen T. C. and Raulin F. (2010) Composition of Titan's lower atmosphere and simple surface volatiles as measured by the Cassini–Huygens probe gas chromatograph mass spectrometer experiment. *J. Geophys. Res.* **115**, E12006. http://dx.doi.org/10.1029/2010JE003659.

Omar M. H., Dokoupil Z. and Schroten H. G. M. (1962) Determination of the solid–liquid equilibrium diagram for the nitrogen–methane system. *Physica* **28**, 309–329.

Parrish W. R. and Hiza M. J. (1974) Liquid–vapor equilibria in the nitrogen–methane system between 95 and 120 K. *Adv. Cryog. Eng.* **19**, 300–308.

Peng D. Y. (2010) Extending the van Laar model to multicomponent systems. *Open Thermodyn. J.* **4**, 129–140.

Penteado P. F. and Griffith C. A. (2010) Ground-based measurements of the methane distribution on Titan. *Icarus* **206**, 345–351.

Pitzer K. S. (1973) Thermodynamics of electrolytes. I. Theoretical basis and general equations. *J. Phys. Chem.* **77**, 268–277.

Poling B. E., Prausnitz J. M. and O'Connell J. P. (2001) *The Properties of Gases and Liquids*. McGraw-Hill, New York.

Poon D. P. L. and Lu B. C. Y. (1974) Phase equilibria for systems containing nitrogen, methane, and propane. *Adv. Cryog. Eng.* **19**, 292–299.

Prausnitz J. M., Lichtenthaler R. N. and Gomes de Azevedo E. (1999) *Molecular Thermodynamics of Fluid-Phase Equilibria*. Prentice Hall PTR, Upper Saddle River, New Jersey.

Preston G. T. and Prausnitz J. M. (1970) Thermodynamics of solid solubility in cryogenic solvents. *Ind. Eng. Chem. Process Des. Dev.* **9**, 264–271.

Raulin F. (1987) Organic chemistry in the oceans of Titan. *Adv. Space Res.* **7**, 71–81.

Robb L. (2005) *Introduction to Ore-Forming Processes*. Blackwell Publishing, Malden, MA.

Samuelson R. E., Nath N. R. and Borysow A. (1997) Gaseous abundances and methane supersaturation in Titan's troposphere. *Planet. Space Sci.* **45**, 959–980.

Scatchard G. (1931) Equilibria in non-electrolyte solutions in relation to the vapor pressures and densities of the components. *Chem. Rev.* **8**, 321–333.

Schindler D. L., Swift G. W. and Kurata F. (1966) More low temperature V-L design data. *Hydrocarbon Process.* **45**, 205–210.

Schneider T., Graves S. D. B., Schaller E. L. and Brown M. E. (2012) Polar methane accumulation and rainstorms on Titan from simulations of the methane cycle. *Nature* **481**, 58–61.

Setzmann U. and Wagner W. (1991) A new equation of state and tables of thermodynamic properties for methane covering the range from the melting line to 625 K at pressures up to 1000 MPa. *J. Phys. Chem. Ref. Data* **20**, 1061–1155.

Shock E. L., Helgeson H. C. and Sverjensky D. A. (1989) Calculation of the thermodynamic and transport properties of aqueous species at high pressures and temperatures: standard partial molal properties of inorganic neutral species. *Geochim. Cosmochim. Acta* **53**, 2157–2183.

Smukala J., Span R. and Wagner W. (2000) New equation of state for ethylene covering the fluid region for temperatures from the melting line to 450 K at pressures up to 300 MPa. *J. Phys. Chem. Ref. Data* **29**, 1053–1121.

Soderblom L. A., Tomasko M. G., Archinal B. A., Becker T. L., Bushroe M. W., Cook D. A., Doose L. R., Galuszka D. M., Hare T. M., Howington-Kraus E., Karkoschka E., Kirk R. L., Lunine J. I., McFarlane E. A., Redding B. L., Rizk B., Rosiek M. R., See C. and Smith P. H. (2007) Topography and geomorphology of the Huygens landing site on Titan. *Planet. Space Sci.* **55**, 2015–2024.

Soderblom J. M., Barnes J. W., Soderblom L. A., Brown R. H., Griffith C. A., Nicholson P. D., Stephan K., Jaumann R., Sotin C., Baines K. H., Buratti B. J. and Clark R. N. (2012) Modeling specular reflections from hydrocarbon lakes on Titan. *Icarus* **220**, 744–751.

Span R., Lemmon E. W., Jacobsen R. T., Wagner W. and Yokozeki A. (2000) A reference equation of state for the thermodynamic properties of nitrogen for temperatures from 63.151 to 1000 K and pressures to 2200 MPa. *J. Phys. Chem. Ref. Data* **29**, 1361–1433.

Sprow F. B. and Prausnitz J. M. (1966) Vapor–liquid equilibria for five cryogenic mixtures. *Am. Inst. Chem. Eng. J.* **12**, 780–784.

Stephan K., Jaumann R., Brown R. H., Soderblom J. M., Soderblom L. A., Barnes J. W., Sotin C., Griffith C. A., Kirk R. L., Baines K. H., Buratti B. J., Clark R. N., Lytle D. M., Nelson R. M. and Nicholson P. D. (2010) Specular reflection on Titan: liquids in Kraken Mare. *Geophys. Res. Lett.* **37**, L07104. http://dx.doi.org/10.1029/2009GL042312.

Stoeckli H. F. and Staveley L. A. K. (1970) Low temperature thermodynamics: the excess Gibbs function and the volumes of mixing for the system methane + propane at 90.68 K. *Helv. Chim. Acta* **53**, 1961–1964.

Stofan E. R., Elachi C., Lunine J. I., Lorenz R. D., Stiles B., Mitchell K. L., Ostro S., Soderblom L., Wood C., Zebker H., Wall S., Janssen M., Kirk R., Lopes R., Paganelli F., Radebaugh J., Wye L., Anderson Y., Allison M., Boehmer R., Callahan P., Encrenaz P., Flamini E., Francescetti G., Gim Y., Hamilton G., Hensley S., Johnson W. T. K., Kelleher K., Muhleman D., Paillou P., Picardi G., Posa F., Roth L., Seu R., Shaffer S., Vetrella S. and West R. (2007) The lakes of Titan. *Nature* **445**, 61–64.

Stofan E. R., Lunine J. I., Lorenz R. D., Aharonson O., Bierhaus E., Clark B., Griffith C., Harri A.- M., Karkoschka E., Kirk R., Kantsiper B., Mahaffy P., Newman C., Ravine M., Trainer M., Waite H. and Zarnecki J. (2010) Exploring the seas of Titan: The Titan Mare Explorer (TiME) mission. *Lunar Planet. Sci. Conf.* #1236 (abstr.).

Strobel D. F., Atreya S. K., Bezard B., Ferri F., Flasar F. M., Fulchignoni M., Lellouch E. and Muller-Wodarg I. (2009) Atmospheric structure and composition. In *Titan from Cassini–Huygens*. Springer, New York, pp. 235–257.

Stryjek R., Chappelear P. S. and Kobayashi R. (1974) Low-temperature vapor–liquid equilibria of nitrogen–methane system. *J. Chem. Eng. Data* **19**, 334–339.

Stull D. R. (1947) Vapor pressure of pure substances: organic compounds. *Ind. Eng. Chem.* **39**, 517–540.

Summerfield M. A. (1991) *Global Geomorphology: An Introduction to the Study of Landforms*. Pearson, Singapore.

Szczepaniec-Cieciak E., Kondaurov V. A. and Melikova S. M. (1980) Study on the solubility light alkanes in liquid nitrogen. *Cryogenics* **20**, 48–51.

Tan S. P., Kargel J. S. and Marion G. M. (2013) Titan's atmosphere and surface liquid: new calculation using statistical associating fluid theory. *Icarus* **222**, 53–72.

Thompson W. R. (1985) Phase equilibria in N_2-hydrocarbon systems: applications to Titan. In *The Atmospheres of Saturn and Titan* (eds. E. Rolfe and B. Battrick), ESA SP-241. ESA Publ. Div., Noordwijk, Netherlands. pp. 109–119.

Thompson W. R., Calado J. C. G. and Zollweg J. A. (1990) Liquid–vapor equilibrium of multicomponent cryogenic systems. In *First International Conference on Laboratory Research for Planetary Atmospheres* (eds. K. Fox, J. E. Allen, Jr., L. J. Stief and D. T. Quillen), NASA CP-3077. NASA, Washington, D.C. pp. 303–326.

Thompson W. R., Henry T. J., Schwartz J. M., Khare B. N. and Sagan C. (1991) Plasma discharge in $N_2 + CH_4$ at low pressures: experimental results and applications to Titan. *Icarus* **90**, 57–73.

Thompson W. R., Zollweg J. A. and Gabis D. H. (1992) Vapor–liquid equilibrium thermodynamics of $N_2 + CH_4$: model and Titan applications. *Icarus* **97**, 187–199.

Tickner A. W. and Lossing F. P. (1951) The measurement of low vapor pressures by means of a mass spectrometer. *J. Phys. Colloid Chem.* **55**, 733–740.

Tiffin D. L., Kohn J. P. and Luks K. D. (1979) Solid hydrocarbon solubility in liquid methane–ethane mixtures along three-phase solid–liquid–vapor loci. *J. Chem. Eng. Data* **24**, 306–310.

Tokano T. (2009) Impact of seas/lakes on polar meteorology of Titan: simulation by a coupled GCM-Sea model. *Icarus* **204**, 619–636.

Tomasko M. G., Archinal B., Becker T., Bezard B., Bushroe M., Combes M., Cook D., Coustenis A., de Bergh C., Dafoe L. E., Doose L., Doute S., Eibl A., Engel S., Gliem F., Grieger B., Holso R., Howington-Kraus E., Karkoschka E., Keller H. U., Kirk R., Kramm R., Kuppers M., Lanagan P., Lellouch E., Lemmon M., Lunine J., McFarlane E., Moores J., Prout G. M., Rizk B., Rosiek M., Rueffer P., Schroder S. E., Schmitt B., See C., Smith P., Soderblom L., Thomas N. and West R. (2005) Rain, winds and haze during the Huygens probe's descent to Titan's surface. *Nature* **438**, 765–778.

Tosca N. J. and McLennan S. M. (2006) Chemical divides and evaporite assemblages on Mars. *Earth Planet. Sci. Lett.* **241**, 21–31.

TSSM (Titan Saturn System Mission) Final Report on the NASA Contribution to a Joint Mission with ESA. 30 Jan. (2009) Task Order #NMO710851. *Outer Planet Flagship Mission Reports*. 21 Mar. 2012. <http://opfm.jpl.nasa.gov/library>.

Turtle E. P., Perry J. E., McEwen A. S., DelGenio A. D., Barbara J., West R. A., Dawson D. D. and Porco C. C. (2009) Cassini imaging of Titan's high-latitude lakes, clouds, and south-polar surface changes. *Geophys. Res. Lett.* **36**, L02204. http://dx.doi.org/10.1029/2008GL036186.

Turtle E. P., Perry J. E., Hayes A. G., Lorenz R. D., Barnes J. W., McEwen A. S., West R. A., Del Genio A. D., Barbara J. M., Lunine J. I., Schaller E. L., Ray T. L., Lopes R. M. C. and Stofan E. R. (2011a) Rapid and extensive surface changes near Titan's equator: evidence of April showers. *Science* **331**, 1414–1417.

Turtle E. P., Perry J. E., Hayes A. G. and McEwen A. S. (2011b) Shoreline retreat at Titan's Ontario Lacus and Arrakis Planitia from Cassini Imaging Science Subsystem observations. *Icarus* **212**, 957–959.

van Laar J. J. (1906) *Sechs Vorträge über das Thermodynamische Potential (Six Lectures on the Thermodynamic Potential)*. Vieweg & Sohn, Braunschweig, Germany.

Vinatier S., Bezard B., Nixon C. A., Mamoutkine A., Carlson R. C., Jennings D. E., Guandique E. A., Teanby N. A., Bjoraker G. L., Flasar F. M. and Kunde V. G. (2010) Analysis of Cassini/CIRS limb spectra of Titan acquired during the nominal mission: I. Hydrocarbons, nitriles and CO_2 vertical mixing ratio profiles. *Icarus* **205**, 559–570.

Watson A. (1983) Gypsum crusts. In *Chemical Sediments and Geomorphology: Precipitates and Residua in the Near-Surface Environment* (eds. A. S. Goudie and K. Pye). Academic Press, New York, pp. 133–161.

Wichterle I. and Kobayashi R. (1972) Vapor–liquid equilibrium of methane–ethane–propane system at low temperatures and high pressures. *J. Chem. Eng. Data* **17**, 13–18.

Wilson G. M. (1975) Vapor–liquid equilibria of nitrogen, methane, ethane, and propane binary mixtures at LNG temperatures from total pressure measurements. *Adv. Cryog. Eng.* **20**, 164–171.

Wohl K. (1946) Thermodynamic evaluation of binary and ternary liquid systems. *Trans. Am. Inst. Chem. Eng.* **42**, 215–249.

Yu P., Elshayal I. M. and Lu B. C. Y. (1969) Liquid–liquid–vapor equilibria in the nitrogen–methane–ethane system. *Can. J. Chem. Eng.* **47**, 495–498.

Yung Y. L., Allen M. and Pinto J. P. (1984) Photochemistry of the atmosphere of Titan: comparison between model and observations. *Astrophys. J. Suppl. Ser.* **55**, 465–506.

Zhou L., Zheng W., Kaiser R. I., Landera A., Mebel A. M., Liang M.-C. and Yung Y. L. (2010) Cosmic-ray-mediated formation of benzene on the surface of Saturn's moon Titan. *Astrophys. J.* **718**, 1243–1251.

Associate editor: Nicolas Dauphas